

RESEARCH ARTICLE

Conserved properties of *Drosophila* Insomniac link sleep regulation and synaptic function

Qiuling Li¹, David A. Kellner¹, Hayden A. M. Hatch^{1‡}, Tomohiro Yumita¹, Sandrine Sanchez¹, Robert P. Machold¹, C. Andrew Frank^{2,3}, Nicholas Stavropoulos^{1*}

1 Neuroscience Institute, Department of Neuroscience and Physiology, New York University School of Medicine, New York, NY, United States of America, **2** Department of Anatomy and Cell Biology, University of Iowa Carver College of Medicine, Iowa City, IA, United States of America, **3** Interdisciplinary Programs in Genetics, Neuroscience, and MCB, University of Iowa, Iowa City, IA, United States of America

‡ Current address: Department of Neuroscience, Albert Einstein College of Medicine, Bronx, NY, United States of America

* nicholas.stavropoulos@nyumc.org



 OPEN ACCESS

Citation: Li Q, Kellner DA, Hatch HAM, Yumita T, Sanchez S, Machold RP, et al. (2017) Conserved properties of *Drosophila* Insomniac link sleep regulation and synaptic function. PLoS Genet 13 (5): e1006815. <https://doi.org/10.1371/journal.pgen.1006815>

Editor: Amita Sehgal, University of Pennsylvania, UNITED STATES

Received: February 2, 2017

Accepted: May 12, 2017

Published: May 30, 2017

Copyright: © 2017 Li et al. This is an open access article distributed under the terms of the [Creative Commons Attribution License](https://creativecommons.org/licenses/by/4.0/), which permits unrestricted use, distribution, and reproduction in any medium, provided the original author and source are credited.

Data Availability Statement: All relevant data are within the paper and its Supporting Information files.

Funding: This research was supported by an International Student Research Fellowship from the Howard Hughes Medical Institute (QL), by NIH NS062738 and Whitehall Foundation grant 2014-08-03 (CAF), by Whitehall Foundation grant 2013-05-78 and grants from the Alfred P. Sloan, Leon Levy, and Mathers Foundations, a NARSAD Young Investigator Award from the Brain and Behavior

Abstract

Sleep is an ancient animal behavior that is regulated similarly in species ranging from flies to humans. Various genes that regulate sleep have been identified in invertebrates, but whether the functions of these genes are conserved in mammals remains poorly explored. *Drosophila insomniac (inc)* mutants exhibit severely shortened and fragmented sleep. Inc protein physically associates with the Cullin-3 (Cul3) ubiquitin ligase, and neuronal depletion of Inc or Cul3 strongly curtails sleep, suggesting that Inc is a Cul3 adaptor that directs the ubiquitination of neuronal substrates that impact sleep. Three proteins similar to Inc exist in vertebrates—KCTD2, KCTD5, and KCTD17—but are uncharacterized within the nervous system and their functional conservation with Inc has not been addressed. Here we show that Inc and its mouse orthologs exhibit striking biochemical and functional interchangeability within Cul3 complexes. Remarkably, KCTD2 and KCTD5 restore sleep to *inc* mutants, indicating that they can substitute for Inc in vivo and engage its neuronal targets relevant to sleep. Inc and its orthologs localize similarly within fly and mammalian neurons and can traffic to synapses, suggesting that their substrates may include synaptic proteins. Consistent with such a mechanism, *inc* mutants exhibit defects in synaptic structure and physiology, indicating that Inc is essential for both sleep and synaptic function. Our findings reveal that molecular functions of Inc are conserved through ~600 million years of evolution and support the hypothesis that Inc and its orthologs participate in an evolutionarily conserved ubiquitination pathway that links synaptic function and sleep regulation.

Author summary

Sleep is ubiquitous among animals and is regulated in a similar manner across phylogeny, but whether conserved molecular mechanisms govern sleep is poorly defined. The Insomniac protein is vital for sleep in *Drosophila* and is a putative adaptor for the Cul3 ubiquitin ligase. We show that two mammalian orthologs of Insomniac can restore sleep to flies

Research Foundation, a New York University Whitehead Fellowship, and the J. Christian Gillin, M.D. Research Award from the Sleep Research Society Foundation (NS). The funders had no role in study design, data collection and analysis, decision to publish, or preparation of the manuscript.

Competing interests: The authors have declared that no competing interests exist.

lacking Insomniac, indicating that the molecular functions of these proteins are conserved through evolution. Our comparative analysis reveals that Insomniac and its mammalian orthologs can localize to neuronal synapses and that Insomniac impacts synaptic structure and physiology. Our findings suggest that Insomniac and its mammalian orthologs are components of an evolutionarily conserved ubiquitination pathway that links synaptic function and the regulation of sleep.

Introduction

Sleep is an evolutionarily ancient behavior present in vertebrates and invertebrates [1]. The similar characteristics of sleep states across animal phylogeny suggest that both the functions of sleep and the regulation of sleep may have a common evolutionary basis [2]. In diverse animals including mammals and insects, sleep is regulated similarly by circadian and homeostatic mechanisms [3]. The circadian regulation of sleep is better understood at a molecular level, and numerous studies have revealed that the underlying genes and intracellular pathways are largely conserved from flies to humans [4–10]. In contrast, the molecular mechanisms underlying the non-circadian regulation of sleep—including those governing sleep duration, consolidation, and homeostasis—remain less well defined, and their evolutionary conservation is largely unexplored.

Mutations of the *Drosophila insomniac* (*inc*) gene [11] severely curtail the duration and consolidation of sleep but do not alter its circadian regulation [11,12]. *inc* encodes a protein of the Bric-à-brac, Tramtrack, and Broad / Pox virus zinc finger (BTB/POZ) superfamily [13], which includes adaptors for the Cullin-3 (Cul3) E3 ubiquitin ligase complex [14–17]. Cul3 adaptors have a modular structure, in which the BTB domain binds Cul3 and a second distal domain recruits substrates to the Cul3 complex for ubiquitination [14–17]. The BTB domain also mediates adaptor self-association, enabling the oligomerization of Cul3 complexes and the efficient recruitment and ubiquitination of substrates [18,19]. Biochemical and genetic evidence supports the hypothesis that Inc is a Cul3 adaptor [11,12]. Inc and Cul3 physically interact in cultured cells [11,12] and Inc is able to self-associate [12]. In vivo, neuronal RNAi against *inc* or *Cul3* strongly reduces sleep [11,12], and reduction in the levels of Nedd8, a protein whose conjugation to Cullins is essential for their activity, also decreases sleep [11]. While Inc is thus likely to function as a Cul3 adaptor within neurons to promote sleep, the neuronal mechanisms through which Inc influences sleep are unknown.

Three proteins similar to Inc—KCTD2, KCTD5, and KCTD17—are present in vertebrates [11,20,21], but their functions in the nervous system are uncharacterized and their functional conservation with Inc has not been addressed. KCTD5 can self-associate and bind Cul3 [20], suggesting that it may serve as a Cul3 adaptor, yet no substrates have been identified among its interacting partners [22,23]. One KCTD17 isoform has been shown to function as a Cul3 adaptor for trichoplein, a regulator of primary cilia [24]. However, trichoplein-binding sequences are not present in Inc, KCTD2, KCTD5, or other KCTD17 isoforms, and trichoplein is not conserved in *Drosophila*. Thus, it remains unclear whether Inc and its vertebrate homologs have conserved molecular functions, particularly within neurons and cellular pathways relevant to sleep.

Here, we assess the functional conservation of Inc and its mammalian orthologs and elucidate a neuronal mechanism through which they may impact sleep. Inc and each of its orthologs bind Cul3 and self-associate, supporting a universal role for these proteins as Cul3 adaptors. Inc and its orthologs furthermore exhibit biochemical interchangeability within Inc-

Inc and Inc-Cul3 complexes, indicating that the oligomeric architecture of Inc-Cul3 complexes is highly conserved. Strikingly, KCTD2 and KCTD5 can functionally substitute for Inc in vivo and restore sleep to *inc* mutants, indicating that these Inc orthologs readily engage the molecular targets through which Inc impacts sleep. Our studies furthermore reveal that Inc and its orthologs localize similarly within fly and mammalian neurons and are able to traffic to synapses. Finally, we show that *inc* mutants exhibit defects in synaptic structure and physiology, indicating that *inc* is essential for both sleep and synaptic function. Our findings demonstrate that molecular functions of Inc are conserved from flies to mammals, and support the hypothesis that Inc and its orthologs direct the ubiquitination of conserved neuronal proteins that link sleep regulation and synaptic function.

Results

The mammalian orthologs of Insomniac are expressed in the nervous system

Inc functions in neurons to impact sleep [11,12]. To assess whether Inc orthologs are expressed in the mammalian nervous system, we performed RT-PCR on whole adult mouse brain RNA using primers specific for KCTD2, KCTD5, and KCTD17. All three genes are expressed in the brain (Fig 1A), and in situ hybridizations reveal expression within cortex, thalamus, striatum, pons, and cerebellum among other brain regions (S1 Fig). Cloning of RT-PCR products revealed single transcripts for KCTD2 and KCTD5, encoding proteins of 263 and 234 residues respectively, and two alternatively spliced transcripts for KCTD17, encoding proteins of 225 and 220 residues with distinct C-termini (Fig 1B and S2A Fig). These KCTD17 isoforms, KCTD17.2 and KCTD17.3, have not been characterized previously and lack residues of a longer KCTD17 isoform required to bind trichoplein (S2B Fig) [24]. Thus, KCTD17.2 and KCTD17.3 are likely to

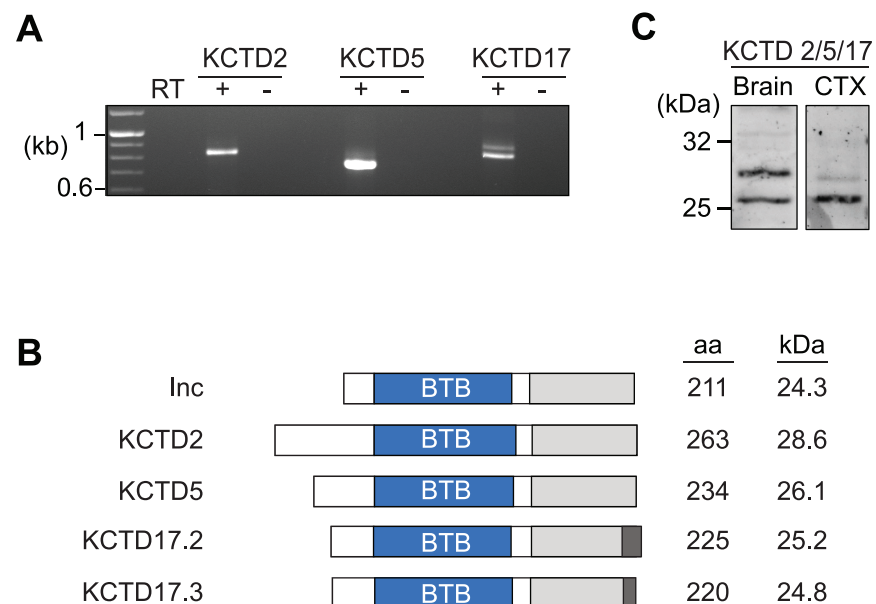


Fig 1. Expression analysis of mammalian Insomniac orthologs. (A) RT-PCR amplification of KCTD2, KCTD5, and KCTD17 from whole adult mouse brain RNA. The presence (+) or absence (-) of reverse transcriptase (RT) prior to PCR is indicated. (B) Structure of Inc family members. Conserved BTB (blue) and C-terminal domains (grey), and variant C-terminal residues resulting from alternative splicing of KCTD17 (dark grey) are shown. Number of amino acid (aa) residues and predicted molecular weights of each protein are indicated. (C) Western blot of whole adult mouse brain and rat cortical culture (CTX) extracts probed with anti-KCTD5 antibody that recognizes KCTD2, KCTD5, and KCTD17.

<https://doi.org/10.1371/journal.pgen.1006815.g001>

have different molecular partners. KCTD17.2 and KCTD17.3 behaved indistinguishably in our experiments except where noted below. Inc and its mouse orthologs share ~60% sequence identity, and have variable N-termini followed by a BTB domain, an intervening linker, and conserved C-termini (S2A Fig) [11,20,21].

We next assessed the expression of KCTD2, KCTD5, and KCTD17 proteins, using a polyclonal anti-KCTD5 antibody that cross-reacts with mouse Inc orthologs and *Drosophila* Inc (S3A Fig). This antibody detected a strongly reactive species of ~26 kD and additional species of ~28 to 29 kD in extracts from mouse and rat brain, cultured rat cortical neurons, and human 293T cells (Figs 1C and 5D, and S3A Fig), consistent with the range of molecular weights predicted for KCTD2, KCTD5, and KCTD17 (Fig 1B). The size of these immunoreactive species and their biochemical properties, described further below, indicate that they correspond to one or more isoforms of KCTD2, KCTD5, and KCTD17. The expression of Inc orthologs in the mammalian brain and Inc in the fly brain [11], together with the similarity of their primary sequences, suggests that Inc defines a protein family that may have conserved functions in the nervous system.

Insomniac family members self-associate and bind Cul3 in an evolutionarily conserved and interchangeable manner

Inc and KCTD5 are able to bind Cul3 and to self-associate [11,12,20], key attributes of BTB adaptors [14–17]. To determine whether these attributes are universal to Inc orthologs and their isoforms expressed in the nervous system, we first examined the physical interactions of these proteins with mouse Cul3. Co-immunoprecipitations revealed that KCTD2, KCTD5, and KCTD17 are able to associate with mouse Cul3 (Fig 2A), with KCTD5 exhibiting stronger or more stable interactions than KCTD2 and KCTD17. Thus, the ability to bind Cul3 is a conserved property of Inc and its mouse orthologs. Epitope-tagged Cul3 also co-immunoprecipitated the endogenous ~26 kD species detected by anti-KCTD5 antibody, confirming that this species represents KCTD5 or another Inc ortholog (S3B Fig).

To assess the extent to which the Inc-Cul3 interface is evolutionarily conserved, we tested whether *Drosophila* Inc is able to associate with mouse Cul3 in a cross-species manner. We observed that fly Inc and mouse Cul3 interact (Fig 2A), indicating that Inc readily assembles into mammalian Cul3 complexes. Conversely, we tested whether mouse KCTD2, KCTD5, and KCTD17 can associate with fly Cul3 in *Drosophila* S2 cells, and observed that each Inc ortholog associated with fly Cul3 in a manner indistinguishable from Inc (Fig 2B). The interchangeable biochemical associations of Inc family members and Cul3 indicate that the Inc-Cul3 interface is functionally conserved from flies to mammals.

Self-association is a critical property of BTB adaptors that enables the oligomerization of Cul3 complexes and that stimulates substrate ubiquitination [18,19]. To test whether Inc orthologs self-associate in a manner similar to Inc [12], we co-expressed FLAG- and Myc-tagged forms of each Inc ortholog in mammalian cells and performed co-immunoprecipitations. KCTD2, KCTD5, and KCTD17 each homomultimerized strongly (Fig 3A). Thus, homo-oligomerization is a shared property of Inc family proteins. The presence of three Inc orthologs in mammals and their likely co-expression in brain regions such as thalamus and cortex (S1 Fig) led us to test whether these proteins can also heteromultimerize. We observed robust heteromeric associations between all pairwise combinations of Inc orthologs (Fig 3A), a property that may enable functional redundancy in vivo or the assembly of functionally distinct complexes. To further probe the multimeric self-associations of Inc family members, we tested whether KCTD2, KCTD5, and KCTD 17 can heteromultimerize with *Drosophila* Inc. We observed that each Inc ortholog associates readily with Inc in both mammalian and

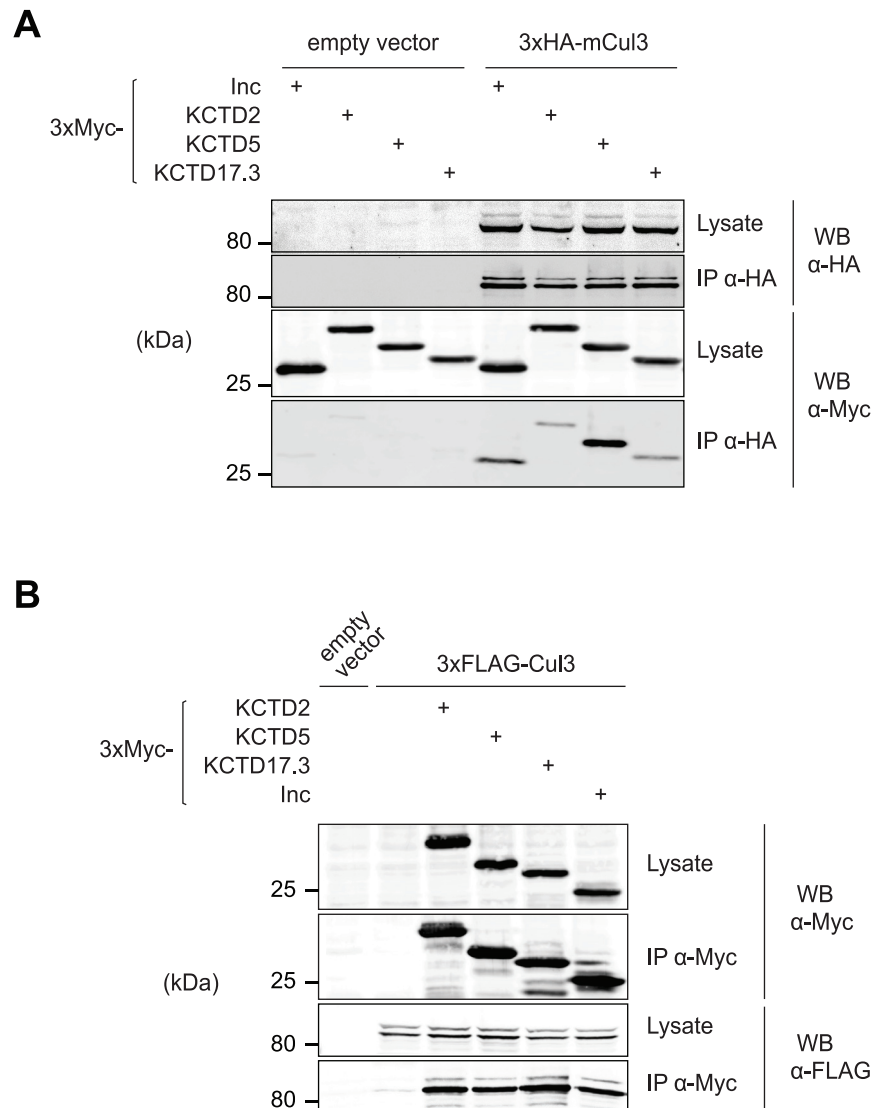


Fig 2. Insomniac-Cul3 interactions are conserved in flies and mammals. (A and B) Co-immunoprecipitation analysis of epitope-tagged Inc or mouse Inc orthologs co-expressed (A) with mouse Cul3 (mCul3) in 293T cells or (B) with *Drosophila* Cul3 in Schneider S2 cells.

<https://doi.org/10.1371/journal.pgen.1006815.g002>

Drosophila cells (Fig 3A and 3B). Thus, the multimerization interface of Inc family members is highly conserved through evolution. Together with the interchangeable associations of Inc family members and Cul3 (Fig 2), these findings strongly suggest a conserved oligomeric architecture for complexes containing Cul3 and Inc family members.

KCTD2 and KCTD5 substitute for *Drosophila* Inc in vivo and restore sleep to *inc* mutants

The biochemical interchangeability of Inc and its mouse orthologs prompted us to test whether Inc function, including its presumed ability to serve as a Cul3 adaptor in vivo and ubiquitinate specific neuronal proteins relevant to sleep, is conserved between flies and mammals. We therefore generated UAS transgenes expressing Myc-tagged forms of Inc, KCTD2, KCTD5, KCTD17.2, and KCTD17.3, integrated each at the *attP2* site [25], and backcrossed these lines to generate an

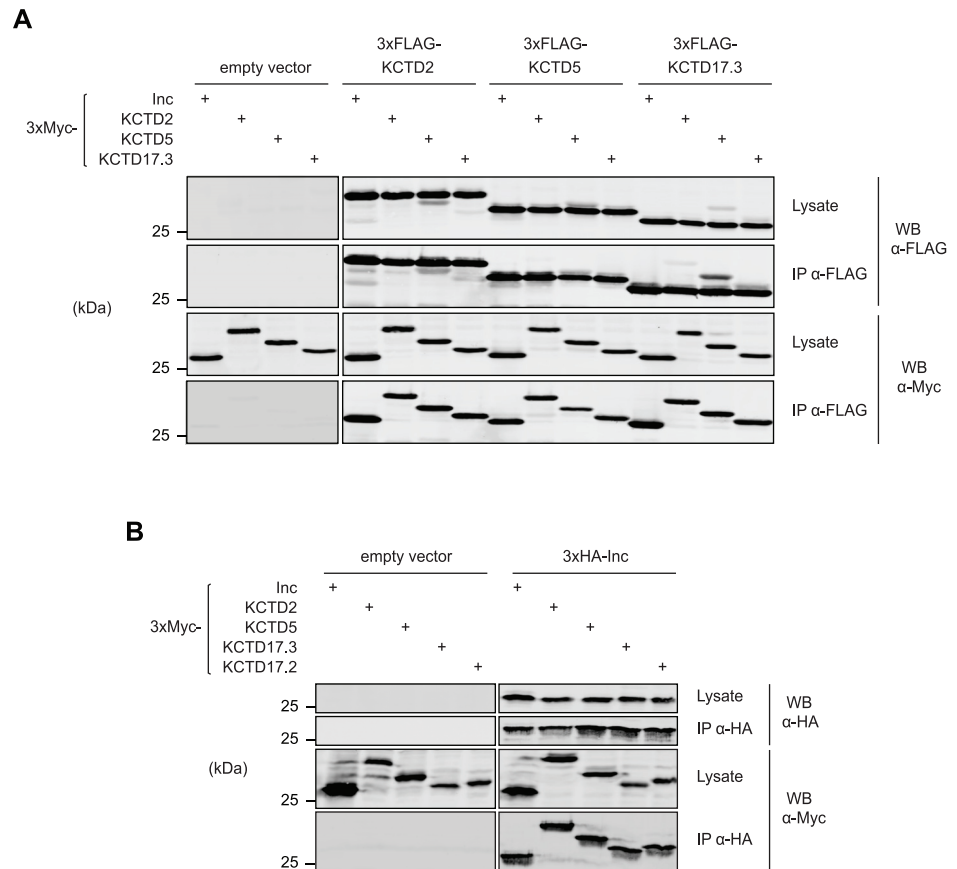


Fig 3. Homomeric and heteromeric interactions of Insomniac family members. (A and B) Co-immunoprecipitation analysis of epitope-tagged Inc and mouse Inc orthologs co-expressed in a pairwise manner in (A) 293T cells or (B) *Drosophila* S2 cells.

<https://doi.org/10.1371/journal.pgen.1006815.g003>

isogenic allelic series. Expression of these transgenes panneuronally with *elav^{c155}-Gal4* yielded similar levels of expression for Inc, KCTD2, and KCTD5, weak expression of KCTD17.2, and low levels of KCTD17.3 expression near the threshold of detection (Fig 4A). Next, we assessed the behavioral consequences of expressing mouse Inc orthologs in vivo. Animals expressing Inc orthologs under the control of *elav^{c155}-Gal4* slept largely indistinguishably from control animals expressing Inc or from those lacking a UAS transgene, as indicated by analysis of sleep duration, daytime and nighttime sleep, sleep bout length, and sleep bout number (Fig 4C and S4A–S4D Fig). Thus, neuronal expression of Inc and its mouse orthologs does not elicit significant dominant negative effects or otherwise inhibit endogenous *inc* function, similar to ubiquitous or neuronal expression of untagged Inc [11].

To assess whether mouse Inc orthologs can functionally substitute for *Drosophila* Inc, we measured their ability to rescue the sleep defects of *inc¹* null mutants [11]. Sleep is a behavior sensitive to genetic background [26,27], environment [28], and other influences, and thus the ability of Inc orthologs to confer behavioral rescue represents a stringent test of *inc* function. Inc and its orthologs expressed under *inc-Gal4* control in *inc¹* animals accumulated with relative levels similar to those in *elav-Gal4* animals (Fig 4A and 4B). Expression of Myc-Inc under *inc-Gal4* control fully rescued sleep in *inc* mutants to wild-type levels, indicating that Myc-Inc recapitulates the function of endogenous Inc protein (Fig 4D). Strikingly, expression of mouse KCTD2 and KCTD5 rescued most of the sleep deficits of *inc* mutants, including those in total

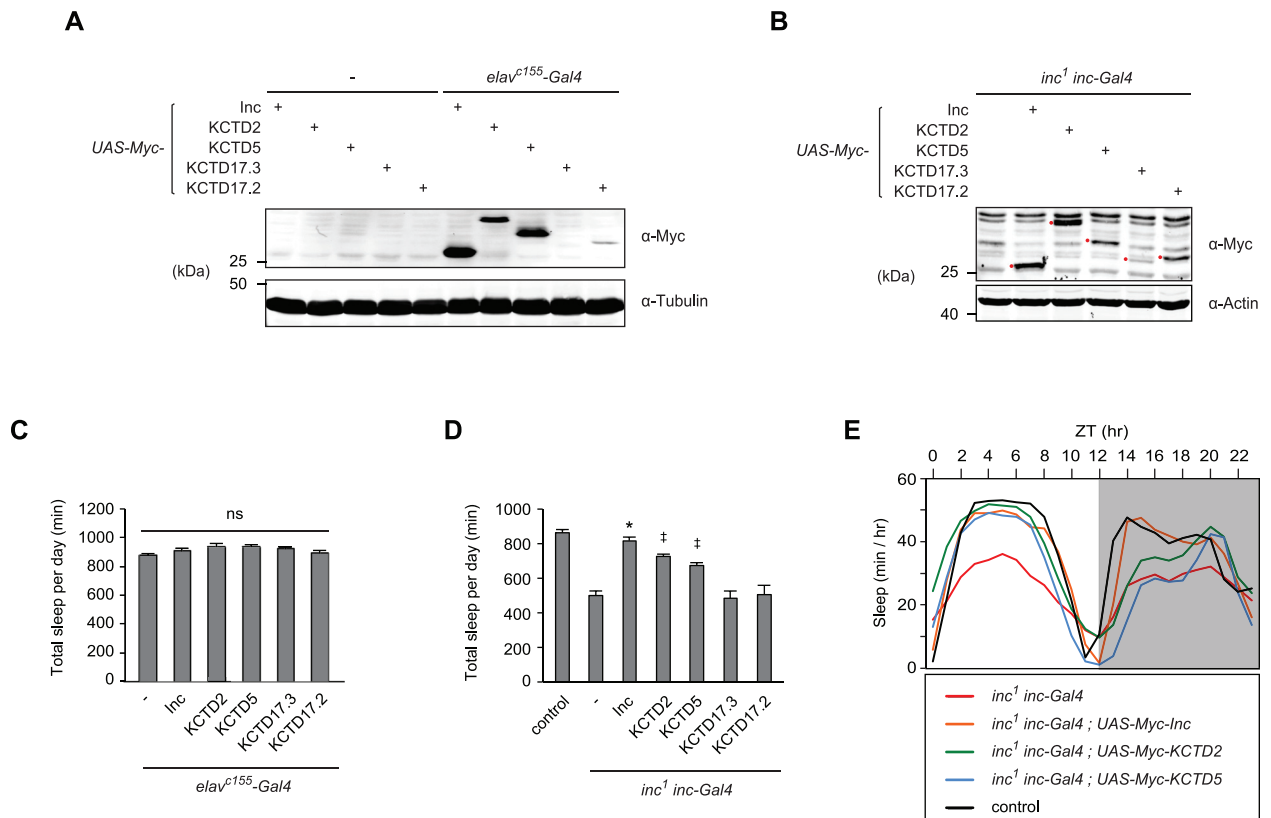


Fig 4. Insomniac orthologs functionally substitute for Insomniac and restore sleep to *inc* mutants in vivo. (A and B) Western blots of head (A) or whole animal lysates (B) prepared from indicated genotypes. Myc-tagged Inc family members are indicated with red dots in (B). (C and D) Total sleep per day for indicated genotypes. Mean \pm SEM is shown. For (C), $n = 37-40$; ns, not significant ($p > 0.05$). For (D) $n = 18-157$; * $p < 0.01$ for comparison to *inc*¹ *inc-Gal4* animals and not significantly different from wild-type controls; † $p < 0.01$ for comparisons to *inc*¹ *inc-Gal4* animals and to wild-type controls. (E) Population average sleep traces summed hourly are shown for indicated genotypes. $n = 56-157$. For all panels, animals are heterozygous for UAS transgenes.

<https://doi.org/10.1371/journal.pgen.1006815.g004>

sleep duration, daytime sleep, sleep bout length, and sleep bout number (Fig 4D and 4E, and S4E–S4H Fig). Nighttime sleep was rescued partially by KCTD2 but not by KCTD5 (S4E Fig). The ability of KCTD2 and KCTD5 to rescue *inc* phenotypes indicates that these proteins not only recapitulate Inc-Inc and Inc-Cul3 interactions (Figs 2 and 3), but also retain other critical aspects of Inc function including its presumed ability to engage and ubiquitinate neuronal target proteins in vivo. In contrast, KCTD17.2 and KCTD17.3 failed to rescue *inc* phenotypes (Fig 4D and S4E–S4H Fig). The restoration of sleep by KCTD2 and KCTD5 but not by isoforms of KCTD17 contrasts with the apparent biochemical interchangeability of these proteins with respect to Inc-Inc and Inc-Cul3 associations (Figs 2 and 3). The inability of KCTD17.2 and KCTD17.3 to rescue *inc* sleep defects may reflect the lower abundance of these proteins in transgenic flies (Fig 4A and 4B) or differences in the intrinsic activities of these KCTD17 isoforms, including their ability to engage Inc targets relevant to sleep.

Insomniac family members traffic through neuronal projections and localize to synapses in mammalian neurons

Inc is required in neurons for normal sleep-wake cycles [11,12], indicating that it impacts aspects of neuronal function that are essential for sleep. The subcellular localization of Cul3 adaptors reflects their biological functions and variously includes the cytoplasm [29], nuclear

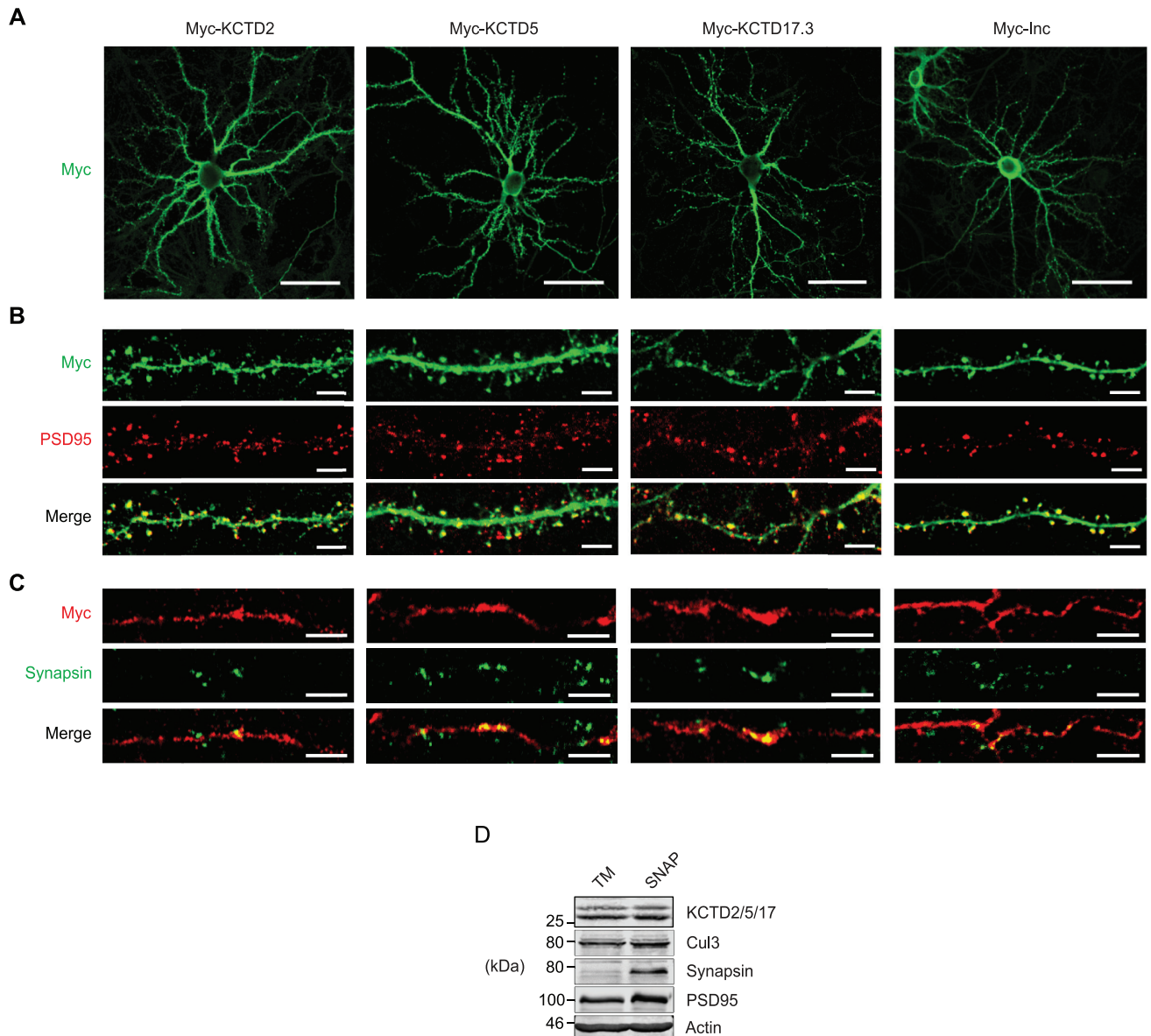


Fig 5. Mammalian *Insomniac* orthologs traffic to neuronal arborizations and synapses. (A–C) Immunohistochemical analysis of rat cortical neurons expressing indicated Myc-tagged proteins. Widefield images of transfected cortical neurons (A), and magnifications of dendrites (B) and axons (C). Scale bars are 50 μ m in (A) and 5 μ m in (B and C). (D) Western blot of total membrane (TM) or synaptosome (SNAP) fractions prepared from rat brain. Note the presence of higher-molecular weight neddylated Cul3.

<https://doi.org/10.1371/journal.pgen.1006815.g005>

foci [30], cytoskeletal structures [31,32], and perisynaptic puncta in neurons [33]. The subcellular distribution of *Inc* is unknown, as available antisera do not efficiently detect endogenous *Inc* [11], and the localization of *Inc* orthologs in neurons is similarly uncharacterized. Anti-KCTD5 antibody did not efficiently detect endogenously expressed *Inc* orthologs in immunohistochemical staining. We therefore examined the subcellular localization of *Inc* family members fused to epitope tags and expressed in cultured cells, primary neurons, and in flies *in vivo*. In S2 cells, Myc-tagged *Inc* was localized to the cytoplasm and excluded from the nucleus (S5A Fig), and an *Inc*-GFP fusion was distributed similarly in both live cells and after fixation (S5A

Fig). Inc orthologs, Inc-GFP, and mouse Cul3 were similarly distributed in the cytoplasm and excluded from the nucleus in cultured mammalian cells (S5B–S5D Fig).

We next assessed the localization of tagged Inc orthologs in primary neurons cultured from cortex, a region of the brain in which they are expressed in vivo (Fig 1C and S1 Fig). In cortical neurons, KCTD2, KCTD5, and KCTD17 were excluded from the nucleus and localized to the cytosol and to dendritic and axonal projections (Fig 5A). Within dendrites, these proteins trafficked to spines as indicated by co-staining against PSD95, a component of the postsynaptic density (Fig 5B). In axons, Inc orthologs were present at varicosities costaining with synapsin, a vesicle-associated protein that marks presynaptic termini (Fig 5C). Inc localized similarly to its mammalian orthologs including at pre- and postsynaptic structures (Fig 5A–5C), suggesting that intrinsic determinants governing the localization of Inc and its orthologs in neurons may be functionally conserved. While the expression of tagged Inc orthologs may not fully recapitulate the abundance or distribution of endogenous proteins, these data suggest that KCTD2, KCTD5, and KCTD17 can localize to various sites within neurons, including the cytosol, projections, and synapses. To further assess whether the localization of Inc orthologs at synapses in transfected neurons reflects the distribution of corresponding endogenous proteins, we fractionated cortex to isolate synaptosomes and subjected them to biochemical analysis. Enrichment of presynaptic and postsynaptic proteins in these preparations was confirmed by blotting for synapsin and PSD95 respectively (Fig 5D). Probing with anti-KCTD5 antibody revealed that Inc orthologs were present in synaptosome fractions (Fig 5D). Similarly, endogenous Cul3 was present in synaptic fractions in its native and higher-molecular weight neddylated form, indicating that active Nedd8-conjugated Cul3 complexes are present at synapses (Fig 5D). Thus, Inc orthologs and Cul3 are present endogenously at mammalian synapses in vivo, suggesting that they form functional ubiquitin ligase complexes at synapses and that their substrates may include synaptic proteins.

Insomniac localizes to the neuronal cytosol, arborizations, and synapses in vivo

To determine whether the localization of Inc in vivo is similar to that of its mouse orthologs, we examined flies expressing Myc-Inc and 3×FLAG-Inc, forms of Inc that rescue the sleep defects of *inc* mutants (Fig 4 and S6 Fig) and which are thus likely to recapitulate attributes of endogenous Inc including its subcellular distribution. In the adult brain, expression of 3×FLAG-Inc under the control of *inc-Gal4* yielded strong anti-FLAG signal in cell bodies and in projections including those of the mushroom bodies, ellipsoid body, and fan-shaped body (Fig 6A). To assess the subcellular localization of Inc in adult neurons more clearly, we first identified sparse neuronal populations likely to express *inc* natively, as indicated by their expression of the *inc-Gal4* driver that fully rescues *inc* mutants (Fig 4D). Animals bearing *inc-Gal4* and a nuclear localized GFP reporter (*UAS-nls-GFP*) exhibited GFP signal in corazonin positive (CRZ⁺) neurons in the dorsal brain [34] and in pigment dispersing factor-expressing (PDF⁺) circadian pacemaker neurons [35] (Fig 6B and S7A Fig). We then utilized Gal4 drivers specific for these neuronal subpopulations to express Myc-Inc and assess its localization. In both populations, Myc-Inc was largely excluded from the nucleus and present in neuronal cell bodies and arborizations (Fig 6C and S7B, S7B' and S7D Fig). To assess the nature of projections containing Inc, we compared the pattern of Inc localization to that of the pre- and postsynaptic markers synaptotagmin-GFP (Syt-eGFP) [36] and DenMark [37] expressed in the same neuronal populations. In corazonin neurons, whose presynaptic and dendritic compartments are well separated, Myc-Inc trafficked both to medial dendritic structures and to lateral puncta located in the same regions as presynaptic termini of these neurons (Fig 6C and 6D–6D"). In

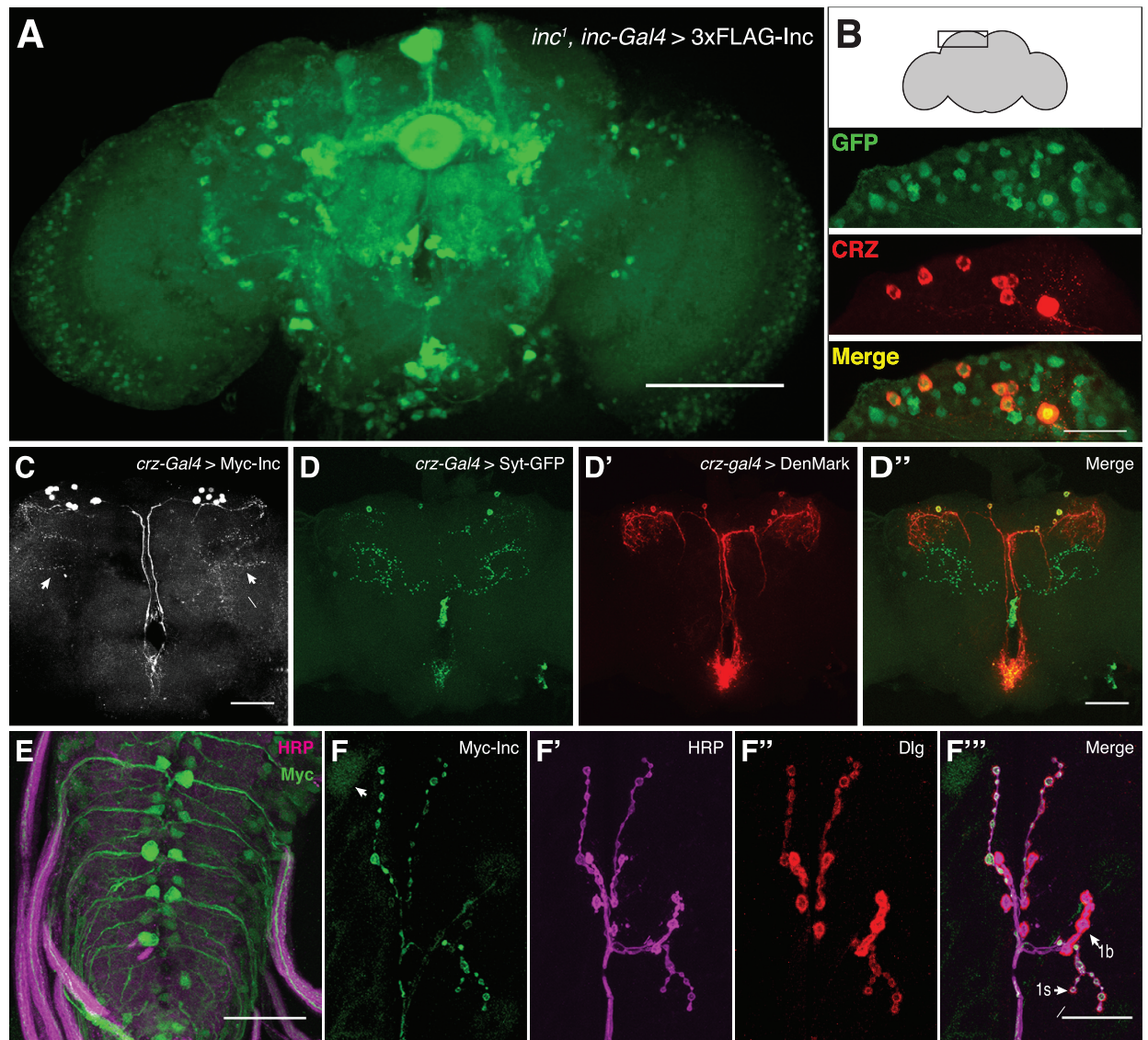


Fig 6. Neuronal localization of Insomniac in vivo. (A–D) Immunohistochemical analysis of adult brains. (A) Maximal Z-projection of *inc¹ inc-Gal4; UAS-3×FLAG-Inc / +* adult brain stained with anti-FLAG. (B) *inc-Gal4; UAS-nls-GFP / +* adult brains stained with anti-GFP and anti-CRZ antibodies. (C) *crz-Gal4 / +; UAS-Myc-Inc / +* brain stained with anti-Myc. Arrows indicate likely presynaptic puncta. (D–D'') *crz-Gal4 / +; UAS-DenMark UAS-Syt-eGFP / +* brain stained with anti-GFP and anti-dsRed antibodies. (E and F–F''') *inc-Gal4 / +; UAS-Myc-Inc / +* third instar larval ventral ganglion (E) and NMJ 6/7 (F) stained with anti-Myc, anti-HRP, and anti-Dlg as indicated. Arrow in (F) indicates weak Myc-Inc signal in muscle nucleus. Scale bars represent 100 μ m in (A), 25 μ m in (B), 50 μ m in (C–E), and 25 μ m in (F).

<https://doi.org/10.1371/journal.pgen.1006815.g006>

PDF⁺ neurons, Myc-Inc was abundant in cell bodies and was detectable in dorsal, ventral, and contralateral projections (S7B, S7B' and S7C–S7C" Fig) [38]. Thus, the localization of Myc-Inc in vivo suggests that Inc may act within the cytosol of neurons as well as their pre- and post-synaptic compartments.

We also assessed Myc-Inc localization in the third instar larval brain and at the larval neuromuscular junction (NMJ), the latter which permits higher resolution analysis of synaptic termini [39]. In animals bearing *inc-Gal4* and *UAS-Myc-Inc*, we observed Inc signal in motor neuron cell bodies and their axonal projections innervating the NMJ (Fig 6E). As in the adult

brain (Fig 6A) [11], Inc expression was present in a subset of neurons, as evident in a fraction of Myc- and HRP-positive projections emanating from the ventral ganglion. At the NMJ itself, Inc was enriched at synaptic boutons and was more prominently expressed within type Is boutons (Fig 6F–6F” and S8A Fig). The presence of Inc in motor neurons, their axonal projections, and at boutons circumscribed by postsynaptic Discs Large (Dlg) signal indicates that Inc signal in these preparations is presynaptic (Fig 6F). Muscle nuclei exhibited weaker Inc signal (Fig 6F–6F”), suggesting, along with comparisons of female and male larvae (S8B Fig), that *inc* may also be expressed postsynaptically at the NMJ. Taken together with findings that Inc orthologs are present at mammalian synapses and have functions conserved with those of Inc (Figs 4 and 5), these data suggest that Inc family members may have evolutionarily conserved functions at synapses.

Altered synaptic anatomy and reduced synaptic strength of *inc* mutants suggest that Inc family proteins may link synaptic function and sleep

A prominent hypothesis invokes synaptic homeostasis as a key function of sleep [40], and findings from vertebrates and flies support the notion that sleep modulates synaptic structure [e.g. 41–45]. Neuronal *inc* activity is essential for normal sleep [11,12], but whether *inc* impacts synaptic function is not known. To test whether the distribution of Inc at synaptic termini reflects a synaptic function, we assessed the anatomical and physiological properties of *inc* mutants at the NMJ. *inc*¹ and *inc*² null mutants both exhibited significantly increased bouton number with respect to wild-type animals (Fig 7A and 7B), indicating that Inc is essential for regulation of synaptic growth or plasticity. To assess whether these anatomical defects are associated with

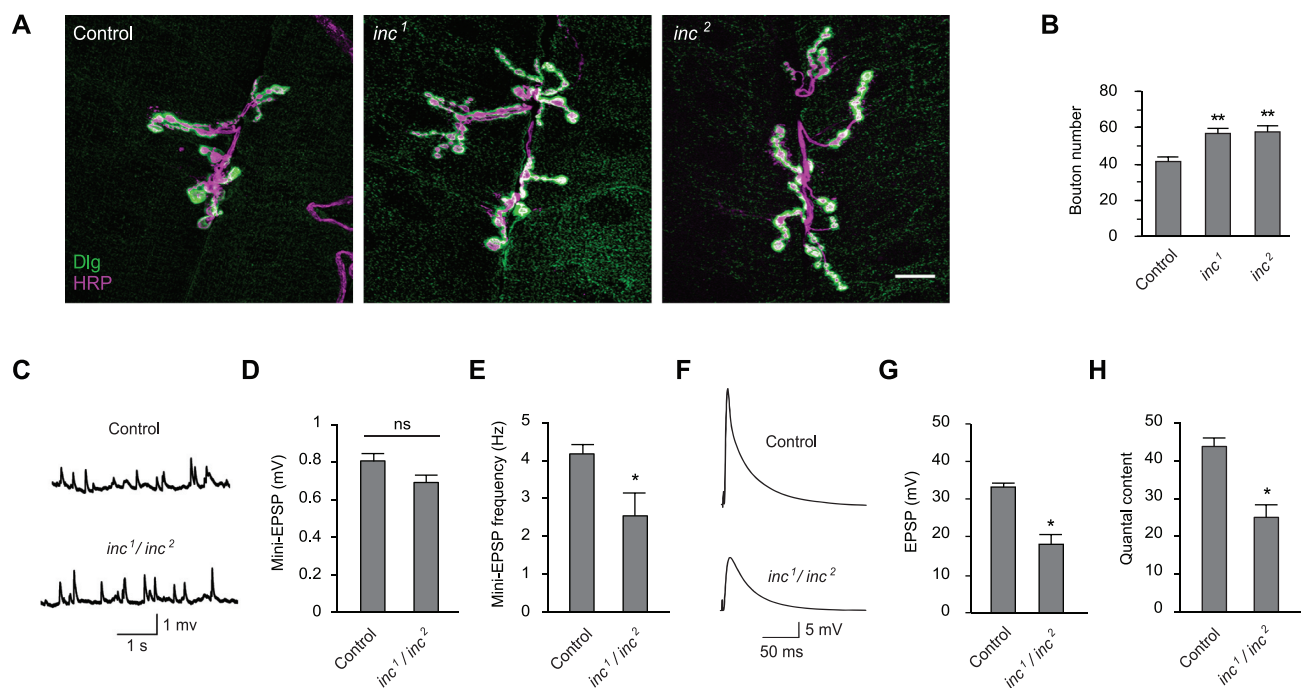


Fig 7. Insomniac is essential for synaptic anatomy and function. (A) Female third instar larval abdominal segment 3 muscle 6/7 NMJ are shown from *inc* mutant or isogenic control *w*¹¹¹⁸ animals. Scale bar is 10 μm. (B) Total bouton count for indicated genotypes at third instar larval abdominal segment 3 muscle 6/7 NMJ. (C) Representative traces of miniature EPSPs for control *w*¹¹¹⁸ and *inc*¹/*inc*² animals. (D) mEPSP amplitude. (E) mEPSP frequency. (F) Representative traces of evoked potentials. (G) EPSP amplitude. (H) Quantal content. For (B), n = 40–43, ** p < 0.001 with respect to control. For (D, E, G, and H), n = 11–31, * p < 0.01; ns, not significant (p > 0.05). For all charts, mean ± SEM is shown.

<https://doi.org/10.1371/journal.pgen.1006815.g007>

altered synaptic transmission, we recorded postsynaptically from muscle in control and trans-heterozygous *inc¹/inc²* animals. While the amplitude of spontaneous miniature postsynaptic potentials was not significantly altered in *inc* mutants, their frequency was reduced (Fig 7C–7E). The amplitude of evoked postsynaptic potentials triggered by presynaptic stimulation was significantly reduced in *inc¹/inc²* mutants, and quantal content was similarly decreased (Fig 7F–7H). The attenuation of evoked potentials and increased bouton number in *inc* mutants suggest that a compensatory increase in synaptic growth may arise in response to defects in synaptic transmission, though this increase does not compensate for the decreased strength of *inc* synapses. These data indicate that *inc* is vital for normal synaptic structure and physiology and suggest, together with the ability of Inc and its orthologs to localize to synapses, that Inc family members may direct the ubiquitination of proteins critical for synaptic function.

Discussion

The presence of sleep states in diverse animals has been suggested to reflect a common purpose for sleep and the conservation of underlying regulatory mechanisms [46]. Here we have shown that attributes of the Insomniac protein likely to underlie its impact on sleep in *Drosophila*—its ability to function as a multimeric Cul3 adaptor and engage neuronal targets that impact sleep—are functionally conserved in its mammalian orthologs. Our comparative analysis of Inc family members in vertebrate and invertebrate neurons furthermore reveals that these proteins can traffic to synapses and that Inc itself is essential for normal synaptic structure and excitability. These findings support the hypothesis that Inc family proteins serve as Cul3 adaptors and direct the ubiquitination of conserved neuronal substrates that impact sleep and synaptic function.

The ability of KCTD2 and KCTD5 to substitute for Inc in the context of sleep is both surprising and notable given the complexity of sleep-wake behavior and the likely functions of these proteins as Cul3 adaptors. Adaptors are multivalent proteins that self-associate, bind Cul3, and recruit substrates, and these interactions are further regulated by additional post-translational mechanisms [47]. Our findings indicate that KCTD2 and KCTD5 readily substitute for Inc within oligomeric Inc-Cul3 complexes, and strongly suggest that these proteins recapitulate other aspects of Inc function in vivo including the ability to engage neuronal targets that impact sleep. The simplest explanation for why KCTD2 and KCTD5 have retained the apparent ability to engage Inc targets despite the evolutionary divergence of *Drosophila* and mammals is that orthologs of Inc targets are themselves conserved in mammals. This inference draws support from manipulations of *Drosophila* Roadkill/HIB and its mammalian ortholog SPOP, Cul3 adaptors of the MATH-BTB family that regulate the conserved Hedgehog signaling pathway [48]. While the ability of SPOP to substitute for HIB has not been assessed by rescue at an organismal level, clonal analysis in *Drosophila* indicates that ectopically expressed mouse SPOP can degrade the endogenous HIB substrate Cubitus Interruptus (Ci), and conversely, that HIB can degrade mammalian Gli proteins that are the conserved orthologs of Ci and substrates of SPOP [48]. By analogy, Inc targets that impact sleep are likely to have orthologs in vertebrates that are recruited by KCTD2 and KCTD5 to Cul3 complexes. While our manipulations do not resolve whether KCTD17 can substitute for Inc in vivo, the ability of KCTD17 to assemble with fly Inc and Cul3 suggests that functional divergence among mouse Inc orthologs may arise outside of the BTB domain, and in particular may reflect properties of their C-termini including the ability to recruit substrates.

The finding that Inc can transit to synapses and is required for normal synaptic function is intriguing in light of hypotheses that invoke synaptic homeostasis as a key function of sleep [40]. While ubiquitin-dependent mechanisms contribute to synaptic function and plasticity

[49–52] and sleep is known to influence synaptic remodeling in both vertebrates and invertebrates [41–45], molecular links between ubiquitination, synapses, and sleep remain poorly explored. Other studies in flies have indicated that regulation of RNA metabolism may similarly couple synaptic function and the control of sleep [53,54]. Alterations in the activity of the Fragile X mental retardation protein (FMR), a regulator of mRNA translation, cause defects in the elaboration of neuronal projections and the formation of synapses as well as changes in sleep duration and consolidation [53,55,56]. Loss of *Adar*, a deaminase that edits RNA, leads to increased sleep through altered glutamatergic synaptic function [54]. Like *Inc*, these proteins are conserved in mammals, suggesting that further studies in flies may provide insights into diverse mechanisms by which sleep influences synaptic function and conversely, how changes in synapses may impact the regulation of sleep.

Our findings at a model synapse suggest that the impact of *Inc* on synaptic function may be intimately linked to its influence on sleep but do not yet resolve important aspects of such a mechanism. The synaptic phenotypes of *inc* mutants—increased synaptic growth, decreased evoked neurotransmitter release, and modest effects on spontaneous neurotransmission—are qualitatively distinct from those of other short sleeping mutants. *Shaker* (*Sh*) and *Hyperkinetic* (*Hk*) mutations decrease sleep in adults [26,57] but increase both excitability and synaptic growth at the NMJ [58–60], suggesting that synaptic functions of *Inc* may affect sleep by a mechanism different than broad neuronal hyperexcitability. While a parsimonious model is that *Inc* directs the ubiquitination of a target critical for synaptic transmission both at the larval NMJ and in neuronal populations that promote sleep, this hypothesis awaits the elucidation of *Inc* targets, definition of the temporal requirements of *Inc* activity, and further mapping of the neuronal populations through which *Inc* impacts sleep [11,12,61]. Finally, determining the localization of endogenous *Inc* within neurons is essential to distinguish possible presynaptic and postsynaptic functions of *Inc* and whether *Inc* engages local synaptic proteins or extrasynaptic targets that ultimately influence synaptic function.

A clear implication of our findings is that neuronal targets and synaptic functions of *Inc* may be conserved in other animals. While the impact of *Inc* orthologs on sleep in vertebrates is as yet unknown, findings from *C.elegans* support the notion that conserved molecular functions of *Inc* and *Cul3* may underlie similar behavioral outputs in diverse organisms. *INSO-1/C52B11.2*, the only *C.elegans* ortholog of *Inc*, interacts with *Cul3* [14], and RNAi against *Cul3* and *INSO-1* reduces the duration of *lethargus*, a quiescent sleep-like state, suggesting that effects of *Cul3*- and *Inc*-dependent ubiquitination on sleep may be evolutionarily conserved [62]. The functions of *Inc* orthologs and *Cul3* in the mammalian nervous system await additional characterization, but emerging data suggest functions relevant to neuronal physiology and disease. Human mutations at the *KCTD2/ATP5H* locus are associated with Alzheimer's disease [63], and mutations of *KCTD17* with myoclonic dystonia [64]. *Cul3* lesions have been associated in several studies with autism spectrum disorders [65–67] and comorbid sleep disturbances [67]. More generally, autism spectrum disorders are commonly associated with sleep deficits [68] and are thought to arise in many cases from altered synaptic function [69], but molecular links to sleep remain fragmentary. Studies of *Inc* family members and their conserved functions in neurons are likely to broaden our understanding of how ubiquitination pathways may link synaptic function to the regulation of sleep and other behaviors.

Methods

RT-PCR and in situ hybridization

Total RNA was isolated with TRIZOL (ThermoFisher) from a single brain hemisphere of a mixed C57BL/6 background adult mouse. 5 µg total RNA was annealed to random hexamer

primers and reverse transcribed with ThermoScript (ThermoFisher) according to the manufacturer's protocol. KCTD2, KCTD5, and KCTD17 transcripts were amplified using primer pairs oNS286 and oNS287, oNS288 and oNS289, and oNS290 and oNS291, respectively.

For in situ hybridization, DNA templates bearing a terminal SP6 promoter for in vitro transcription were generated by PCR amplification of C57BL/6 mouse genomic DNA, using primer pairs oNS1204 and oNS1205 for KCTD2, oNS1207 and oNS1208 for KCTD5, and oNS1213 and oNS1214 for KCTD17. Riboprobes were transcribed with SP6 polymerase and DIG-11-UTP or Fluorescein-12-UTP (Roche). In situ hybridization was performed as described [70], amplifying Fluorescein- and DIG-labeled probes with Fluorescein-tyramide and Cy5-tyramide (Perkin Elmer) respectively.

Plasmids and molecular cloning

Vectors for *Drosophila* transgenesis were as follows:

pUASTattB-Myc-Inc (pNS346) encodes a N-terminal 1×Myc epitope (MEQKLISEEDLAS) fused to Inc, and was generated by three piece ligation of BglII-XhoI digested pUASTattB [71], a BglII-NheI 1×Myc fragment generated by phosphorylating and annealing oligonucleotides oNS283 and oNS284, and an NheI-XhoI *inc* fragment liberated from the PCR amplification product of pUAST-Inc (pNS272) [11] template and primers oNS277 and oNS285.

pUASTattB-Myc-KCTD2 (pNS347) was generated similarly to pNS346, substituting a NheI-XhoI KCTD2 fragment liberated from the PCR amplification product of mouse brain cDNA and primers oNS286 and oNS287. Amplified KCTD2 sequences are identical to those within GenBank accession NM_183285.3.

pUASTattB-Myc-KCTD5 (pNS348) was generated similarly to pNS346, substituting a NheI-XhoI KCTD5 fragment liberated from the PCR amplification product of mouse brain cDNA and primers oNS288 and oNS289. Amplified KCTD5 sequences are identical to those within GenBank accession NM_027008.2.

pUASTattB-Myc-KCTD17.3 (pNS349) and pUASTattB-Myc-KCTD17.2 (pNS350) were generated similarly to pNS346, substituting NheI-XhoI KCTD17 fragments liberated from the PCR amplification products of mouse brain cDNA and primers oNS290 and oNS291. The smaller and larger NheI-XhoI fragments respectively corresponding to KCTD17.3 and KCTD17.2 were gel purified and ligated separately. Amplified KCTD17.3 and KCTD17.2 sequences are identical to those within GenBank accession NM_001289673.1 and NM_001289672.1 respectively.

pUAST-Inc-HA (pNS273) encodes Inc fused to a C-terminal 1×HA epitope (GSYPYDVP-DYA) and was generated by three piece ligation of pUAST BglII-XhoI, a BglII-EcoRI *inc* fragment liberated from pNS272 [11], and an EcoRI-XhoI HA fragment generated by phosphorylating and annealing oligonucleotides oNS191 and oNS192.

pUASTattB-3×FLAG-Inc (pNS404) encodes a N-terminal 3×FLAG epitope (MDYKDDDDKSGSDYKDDDDKAS) fused to Inc and was generated by three piece ligation of EcoRI-XhoI digested pUASTattB, an EcoRI-NheI 3×FLAG fragment liberated from the PCR amplification product of pNS311 template and primers ACF and oNS241, and a NheI-XhoI *inc* fragment liberated from pNS351.

Vectors for expression in S2 cells were as follows:

pAc5.1-3×Myc-Inc (pNS351) encodes a N-terminal 3×Myc epitope (MEQKLISEEDLG-SEQKLISEEDLGSEQKLISEEDLAS) fused to Inc in a derivative of pAc5.1/V5-HisA (ThermoFisher), and was generated by ligating NheI-XhoI digested pNS309 [11] to a NheI-XhoI *inc* fragment prepared as for pNS346.

pAc5.1-3×Myc-KCTD2 (pNS352) was generated similarly to pNS351, substituting a NheI-XhoI KCTD2 fragment prepared as for pNS347.

pAc5.1-3×Myc-KCTD5 (pNS353) was generated similarly to pNS351, substituting a NheI-XhoI KCTD5 fragment prepared as for pNS348.

pAc5.1-3×Myc-KCTD17.3 (pNS391) was generated by ligating NheI-XhoI digested pNS309 to a NheI-XhoI KCTD17.3 fragment liberated from the PCR amplification product of pNS354 template and primers oNS290 and oNS612. pNS354 was generated by ligating NheI-XhoI digested pNS309 and the NheI-XhoI KCTD17.3 fragment prepared as for pNS349.

pAc5.1-3×Myc-KCTD17.2 (pNS392) was generated by ligating NheI-XhoI digested pNS309 to a NheI-XhoI KCTD17.2 fragment liberated from the PCR amplification product of pNS355 template and primers oNS290 and oNS955. pNS355 was generated by ligating NheI-XhoI digested pNS309 and the NheI-XhoI KCTD17.2 fragment prepared as for pNS350.

pAc5.1-3×HA-*Inc* (pNS402) was generated by ligating NheI-XhoI digested pNS310 [11] and a NheI-XhoI *inc* fragment liberated from pNS351.

pAc5.1-3×HA-mCul3 (pNS367) encodes a N-terminal 3×HA epitope (MYPYDVDPDYAG SYPYDVDPDYAGSYPYDVDPDYAAS) fused to mouse Cul3, and was generated by three piece ligation of NheI-NotI digested pNS310 [11], a 0.3 kb NheI-HindIII 5' mCul3 fragment liberated from the PCR amplification product of pCMV-SPORT6-mCul3 template (ThermoFisher, GenBank accession BC027304) and primers oNS313 and oNS314, and a 2.2 kb HindIII-NotI 3' mCul3 fragment generated by digesting pCMV-SPORT6-mCul3 with AvaI, blunting with T4 DNA polymerase, ligating a NotI linker, and digesting with HindIII-NotI.

pAc5.1-3×FLAG-Cul3 (pNS403) encodes a N-terminal 3×FLAG epitope fused to *Drosophila* Cul3 and was generated by ligating NheI-NotI digested pNS311 and a NheI-NotI Cul3 fragment liberated from pNS314 [11]. pNS311 contains a N-terminal 3×FLAG tag and was generated from pNS298, a derivative of pAc5.1/V5-HisA that contains a C-terminal 3×FLAG tag. To construct pNS298, oligonucleotides oNS234 and oNS235 were phosphorylated, annealed, and cloned into XhoI-XbaI digested pAc5.1/V5-HisA. To construct pNS311, the EcoRI-NotI fragment liberated from the PCR amplification product of pNS298 template and primers oNS240 and oNS241 was ligated to EcoRI-NotI digested pAc5.1/V5-HisA.

pAc5.1-*Inc*-GFP (pNS275) encodes *Inc* fused at its C-terminus to GFP and was generated by three piece ligation of EcoRI-NotI digested pAc5.1/V5-HisA, an EcoRI-BamHI *inc* fragment liberated from pNS273, and a BamHI-NotI EGFP fragment liberated from pEGFP-N3 (Clontech).

Mammalian expression vectors were as follows:

pcDNA3.1-3×Myc-*Inc* (pNS358) was generated by ligating NheI-XhoI digested pcDNA3.1 (+) (ThermoFisher) with a SpeI-XhoI 3×Myc-*Inc* fragment liberated from pNS351.

pcDNA3.1-3×Myc-KCTD2 (pNS359) was generated similarly to pNS358, substituting a SpeI-XhoI 3×Myc-KCTD2 fragment liberated from pNS352.

pcDNA3.1-3×Myc-KCTD5 (pNS360) was generated by ligating EcoRI-XhoI digested pcDNA3.1(+) with a EcoRI-XhoI 3×Myc-KCTD5 fragment liberated from pNS353.

pcDNA3.1-3×Myc-KCTD17.3 (pNS393) was generated by three piece ligation of EcoRI-XhoI digested pcDNA3.1(+), an EcoRI-NheI 3×Myc fragment liberated from the PCR amplification product of pNS351 template and primers ACF and oNS318, and a NheI-XhoI KCTD17.3 fragment liberated from the PCR amplification product of pNS354 template and primers oNS290 and oNS612.

pcDNA3.1-3×Myc-KCTD17.2 (pNS394) was generated similarly to pNS393, substituting a NheI-XhoI KCTD17.2 fragment liberated from the PCR amplification product of pNS355 template and primers oNS290 and oNS955.

pcDNA3.1-3×HA-Cul3 (pNS365) was generated by ligating EcoRI-NotI digested pcDNA3.1(+) with the EcoRI-NotI 3×HA-Cul3 fragment from pNS314 [11].

pcDNA3.1–3×HA-mCul3 (pNS369) was generated by ligating KpnI–NotI digested pcDNA3.1(+) with the KpnI–NotI 3×HA-mCul3 fragment liberated from pNS367.

pcDNA3.1–3×FLAG–Inc (pNS395) encodes a N-terminal 3×FLAG epitope fused to Inc, and was generated by three piece ligation of EcoRI–XhoI digested pcDNA3.1(+), an EcoRI–NheI 3×FLAG fragment liberated from the PCR amplification product of pNS386 template and primers ACF and oNS318, and the NheI–XhoI *inc* fragment liberated from pNS351. pNS386 was generated by ligating NheI–XhoI digested pNS311 and an NheI–XhoI *inc* fragment liberated from pNS351.

pcDNA3.1–3×FLAG–KCTD2 (pNS396) was generated similarly to pNS395, substituting an NheI–XhoI KCTD2 fragment liberated from pNS352.

pcDNA3.1–3×FLAG–KCTD5 (pNS397) was generated similarly to pNS395, substituting an NheI–XhoI KCTD5 fragment liberated from pNS353.

pcDNA3.1–3×FLAG–KCTD17.2 (pNS398) was generated similarly to pNS395, substituting the NheI–XhoI fragment liberated from the PCR amplification product of pNS355 template and primers oNS290 and oNS955.

pcDNA3.1–3×FLAG–KCTD17.3 (pNS399) was generated similarly to pNS395, substituting the NheI–XhoI fragment liberated from the PCR amplification product of pNS354 template and primers oNS290 and oNS612.

pEGFPN3–Inc (pNS279) encodes Inc fused at its C-terminus to GFP and was generated by ligating EcoRI–BamHI digested pEGFP–N3 (Clontech) and an EcoRI–BamHI *inc* fragment liberated from pNS273.

Oligonucleotides

Oligonucleotides used in this work are as follows: oNS119 5'-GTCCGCGCGATTCCCTTGC TTGC-3', oNS191 5'-AATTTTGGGAATTGGATCCTACCCCTACGATGTGCCCGATT ACGCCTAAC-3', oNS192 5'-TCGAGTTAGGCGTAATCGGGCACATCGTAGGGGTAG GATCCAATTCCCAA-3', oNS198 5'-ACTGGGATCCATCCGCCTGTGTGGCTGGGAC GG-3', oNS234 5'-TCGAGGCTAGCGACTACAAGGATGATGACGATAAGGGCTCCG ATTACAAGGACGACGATGATAAGGGATCCGATTACAAGGATGATGACGACAAGT GAT-3', oNS235 5'-CTAGATCACTTGTCTGCATCATCCTTGTAATCGGATCCCTTAT CATCGTCGTCCTTGTAAATCGGAGCCCTTATCGTCATCATCCTTGTAGTCGCTAGC C-3', oNS240 5'-ACTGGAATTCGCGGCAACATGGACTACAAGGATGATGACGATA AGGGC-3', oNS241 5'-ACTGGCGGCCGCTCCTAGGGTGCTAGCCTTGTCTGCATCAT CCTTGTAAATCGGAT-3', oNS254 5'-GTGCGCCAAGTGTCTGAAGAACAAGTGG-3', oNS255 5'-GATGAGCTGCCGAGTCAATCGATACAGTC-3', oNS277 5'-ACGTGCTAG CATGAGCACGGTGTTCATAAACTCGC-3', oNS283 5'-GATCTCAACATGGAGCAGA AGCTGATCAGCGAGGAGGATCTGG-3', oNS284 5'-CTAGCCAGATCCTCCTCGCTGA TCAGCTTCTGCTCCATGTTGA-3', oNS285 5'-ACGTGCTAGCTCGAGGGGTTGTGTGT GAATATATAGCGCGA-3', oNS286 5'-ACGTGCTAGCATGGCGGAGCTGCAGCTGG-3', oNS287 5'-ACGTGCTAGCTCGAGCCGCTTACATTCGAGAGCCTCTCTCC-3', oNS288 5'-ACGTGCTAGCATGGCGGAGAATCACTGCGAGCTG-3', oNS289 5'-ACGTGCTAGCTCG AGCCTCACATCCTTGAGCCCCGTTTC-3', oNS290 5'-ACGTGCTAGCATGCAGACAAC GCGGCCGCGC-3', oNS291 5'-ACGTGCTAGCTCGAGCCCAAGGCAGGAGTGAGTCTC AGC-3', oNS313 5'-ACGTGCTAGCATGTGCAATCTGAGCAAAGGCACGGG-3', oNS314 5'-GCCGAAGATGATCCCTAATACCCCATACCG-3', oNS318 5'-ACGTCTCGAGTTACT GCGTCACGTTGTAGAATC-3', oNS612 5'-ACGTCTCGAGTCACATCCGGGTGCCTCT GGCTT-3', oNS955 5'-ACGTCTCGAGTCACTGCAAGCTCAGGCTTGGGTCTG-3', oNS12 04 5'-TAATACGACTCACTATAGGGGAAGGCAAGAGAGCAATCGGC-3', oNS1205 5'-G

CGATTTAGGTGACACTATAGAAGAAAAGGCTGCAGAAGCAGTTAC-3', oNS1207 5'-TAATACGACTCACTATAGGGGGCTCAAGGATGTGAGGAATGCTGAG-3', oNS1208 5'-GCGATTTAGGTGACACTATAGAAGCAGCCTCTATCCCAGGCACAAC-3', oNS1213 5'-TAATACGACTCACTATAGGGTTACAAGCCAGAGGCACCCGGA-3', oNS1214 5'-GC GATTTAGGTGACACTATAGAAGCAGCTCAACCCGTTACACCTGTC-3', ACF 5'-GACA CAAAGCCGCTCCATCAG-3', attP2-5' 5'-CACTGGCACTAGAACAAAAGCTTTGGCG-3'.

Cell culture and biochemistry

293T cells were cultured in DMEM containing 10% FBS, penicillin, and streptomycin, and transfected with Lipofectamine 2000 (ThermoFisher) according to the manufacturers protocol. S2 cells were cultured in S2 media containing 10% FBS, penicillin, and streptomycin, and were transfected with Effectene (Qiagen) as described previously [11]. For both 293T and S2 cells, transfections were performed in 6 well or 12 well plates for ~24h until liposome-containing media was replaced with fresh culture media. Cells or coverslips were harvested for lysis or immunohistochemistry 36-48h after transfections were initiated. For transfections involving more than one plasmid, an equal amount of each was used. Rat cortical neurons were cultured on poly-D-lysine coated coverslips and transfected with calcium phosphate at 7 days in vitro (DIV) as described previously [72].

For co-immunoprecipitations from 293T cells, samples were lysed with ice-cold RIPA buffer (50 mM Tris-Cl pH 7.6, 150 mM NaCl, 50 mM NaF, 2 mM EDTA, 0.5% sodium deoxycholate, 1% NP40, 0.1% SDS) containing protease inhibitor (Sigma, P8340). For co-immunoprecipitation of Inc family members from S2 cells, samples were lysed with ice-cold NP40 buffer (50 mM Tris pH 7.6, 150mM NaCl, 0.5% NP40) containing protease inhibitors or RIPA buffer as above; for S2 cell co-immunoprecipitations involving Cul3, ice-cold NP40 buffer was used. Protein extracts were quantitated in duplicate (BioRad, 5000111) and 160–400 µg (293T) or 800–1000 µg (S2) was immunoprecipitated with 20 µl (50% slurry) of anti-FLAG (Sigma, F2426) or anti-HA (Sigma, E6779) affinity gel for 1 hr nutating at 4°C. Samples were then washed 4×5 min at 4°C with lysis buffer, denatured in SDS sample buffer, separated on Tris SDS-PAGE gels, and transferred to nitrocellulose. Membranes were blocked for 1 hr at room temperature or 4°C overnight in LI-COR Odyssey buffer (LI-COR, 927–40000) or 1% casein in PBS. Membranes were subsequently incubated in blocking buffer containing 0.1% Tween 20 and the appropriate primary antibodies: rabbit anti-Myc (1:2,000, Sigma, C3956), mouse anti-FLAG (1:2,000, Sigma, F1804), rat anti-HA (1:1,000–1:2,000, Roche, 11867431001), rabbit anti-Cul3 (1:1,000, Bethyl Laboratories, A301-109A), and rabbit anti-KCTD5 (1:2,000, Proteintech, 15553-1-AP). After washing 4×5 min in a solution containing 150 mM NaCl, 10mM Tris pH 7.6, and 0.1% Tween 20 (TBST), membranes were incubated in the dark for 30 min at room temperature with appropriate secondary antibodies, all diluted 1:30,000 in blocking buffer containing 0.1% Tween 20 and 0.01% SDS: Alexa 680 donkey anti-rabbit (Life Technologies, A10043), Alexa 790 anti-mouse (Life Technologies, A11371), and Alexa 790 anti-rat (Jackson ImmunoResearch, 712-655-153). Membranes were then washed 4×5 min in TBST, 1×5 min in TBS, and imaged on a Li-Cor Odyssey CLx instrument.

Fly protein extracts were prepared from whole animals or from sieved heads by manual pestle homogenization in ice-cold NP40 lysis buffer supplemented with protease inhibitors. 50 µg was separated on Tris-SDS-PAGE gels and blotted as described above. Primary antibodies were mouse anti-Myc (1:1,000, BioXCell, BE0238; or 1:1,000, Cell Signaling Technology, 2276), rabbit anti-tubulin (1:30,000, VWR, 89364–004), or mouse anti-actin (1:1,000, Developmental Studies Hybridoma Bank (DSHB), JLA20). Secondary antibodies were Alexa 680 donkey anti-

rabbit, Alexa 680 anti-mouse (Life Technologies, A10038), and Alexa 790 anti-rabbit (Life Technologies, A11374).

Mouse and rat brain extracts not used for synaptosome preparations were prepared by homogenizing brains in ice-cold NP40 lysis buffer supplemented with protease inhibitors. Extracts were separated with SDS-PAGE and blotted as described above.

Synaptosomes were prepared from rat brain essentially as described [73], and probed with rabbit anti-Cul3 (1:1,000), mouse anti-Actin (1:1,000), rabbit anti-KCTD5 (1:2,000), guinea-pig anti-synapsin (1:1,000, Synaptic Systems, 106 004), and mouse anti-PSD95 (1:1,000, Neuromab, 75–028). Alexa 680 and Alexa 790 secondary antibodies were used as described above.

Immunohistochemistry and microscopy

Rat cortical neurons transfected at 7 DIV were processed at 13 DIV for immunohistochemistry. Samples were fixed for 15 min with ice-cold 4% paraformaldehyde in Dulbecco's PBS containing 4 mM EGTA and 4% sucrose, and subsequently permeabilized for 10 min in PBS containing 0.5% normal donkey serum (Lampire Biological, 7332100) and 0.1% Triton X-100. Samples were then blocked at room temperature for 30 min in PBS containing 7.5% normal donkey serum and 0.05% Triton X-100, incubated overnight at 4°C in primary antibody cocktail prepared in PBS containing 5% normal donkey serum and 0.05% Triton X-100, and washed 3×5 min in PBS at room temperature. Secondary antibody cocktails were prepared similarly and incubated with samples at room temperature for 30–40 min in the dark. Samples were then washed 3×5 min in PBS at room temperature and mounted on microscope slides in Vectashield (Vector Labs, H-1000). Primary antibodies were rabbit anti-Myc (1:200), mouse anti-PSD95 (1:1,000), and guinea pig anti-synapsin (1:1,000). Secondary antibodies, all diluted at 1:1,000, were Alexa 488 donkey anti-rabbit (Life Technologies, A21206), Alexa 488 donkey anti-guinea pig (Jackson ImmunoResearch, 706-545-148), Alexa 568 donkey anti-mouse (Life Technologies, A10037), and Alexa 568 donkey anti-rabbit (Life Technologies, A10042).

Immunohistochemistry for 293T cells was performed similarly; cells were plated on poly-L-lysine treated coverslips and cultured and transfected as described above. 0.4 µg/ml DAPI was included in the penultimate wash prior to mounting coverslips on microscope slides.

For immunohistochemistry of adult fly brains, whole animals were fixed with 4% paraformaldehyde in PBS containing 0.2% Triton X-100 (PBST) for 3 hr at 4°C, and subsequently washed 3×15 min at room temperature with PBST. Brains were dissected in ice-cold PBST, incubated for 30 min at room temperature in blocking solution containing PBST and 5% normal donkey serum, and incubated overnight at 4°C in primary antibody cocktail diluted in blocking solution. After 3×15 min washes in PBST at room temperature, samples were incubated in secondary antibody cocktail in blocking solution for 1–3 days at 4°C, washed 3×15 min at room temperature with PBST, and mounted on microscope slides in Vectashield. Primary antibodies were mouse anti-FLAG (1:100), rabbit anti-GFP (1:3,000; Life Technologies, A11122), mouse anti-GFP (1:1,000, DSHB, G1), mouse anti-PDF (1:1,000, DSHB, C7), rabbit anti-CRZ (1:1,000, [74]), rabbit anti-DsRed (1:1,000, Clontech, 632496), mouse anti-Myc (1:100, BioXCell, BE0238), and rabbit anti-Myc (1:500, Sigma, C3956). Secondary antibodies, all used at 1:1,000, were Alexa 488 donkey anti-mouse (Life Technologies, A21202), Alexa 488 donkey anti-rabbit, Alexa 568 donkey anti-mouse, and Alexa 568 donkey anti-rabbit.

For immunohistochemistry of larval brains and neuromuscular junctions, wandering third instar larvae were dissected in PBS and pinned to 35mm Sylgard-coated petri dishes. Where experiments required larvae of a specific sex, gonads were identified prior to dissection by visual inspection of animals under PBS immersion as described [75]. Larval filets were fixed for 30 min at room temperature in 4% paraformaldehyde in PBS, and subsequently rinsed

twice and washed 3×20 min in PBST. Samples were blocked in 5% normal donkey serum in PBST at room temperature for 30 min and incubated overnight at 4°C in primary antibody cocktail diluted in blocking solution. Samples were then washed 3×20 min in PBST at room temperature and incubated overnight at 4°C with secondary antibody cocktail in blocking solution, washed, and mounted in Vectashield. Primary antibodies were rabbit anti-myc (1:500), mouse anti-Dlg (1:1,000, DSHB, 4F3), and Alexa 647 goat anti-HRP (1:200, Jackson ImmunoResearch, 123-605-021). Secondary antibodies, used at 1:1000, were Alexa 488 donkey anti-rabbit and Alexa 568 donkey anti-mouse. Neuromuscular junctions were imaged with a confocal microscope and z-stacks were captured using 40× or 63× oil objectives at 512×512 resolution. Boutons were counted offline using a manual tally counter while manipulating z-stacks in 3-dimensional space using Zen software (Zeiss); each axon branch was counted separately to avoid undercounting or duplicate counts and counts were performed three times to ensure consistency. All bouton counting was performed in a double-blind manner with codes revealed after the entire experiment was scored.

For live imaging of Inc-GFP in S2 cells, cells were cultured on poly-L-lysine coated coverslips and transfected with Effectene as described above. 48 hours post-transfection, coverslips were inverted onto a drop of PBS on microscope slides and imaged immediately (within 5 minutes) on a confocal microscope. For imaging of fixed Inc-GFP signal in S2 cells, coverslips were washed twice with PBS, fixed for 25 min in PBS containing 4% paraformaldehyde, washed twice in PBS, and inverted onto drops of Vectashield containing DAPI (Vector) on microscope slides.

All imaging was performed on Zeiss LSM510 or LSM800 confocal microscopes.

Fly stocks and transgenes

elav^{c155}-Gal4 [76] and *inc¹*, *inc²*, and *inc-Gal4* [11] have been described previously. Unless noted otherwise, all experiments were performed with the X-linked *inc-Gal4* transgene. The *inc¹ inc-Gal4* stock was generated by meiotic recombination between isogenic *inc¹* and *inc-Gal4* chromosomes and verified with duplex PCR using primers oNS254 and oNS255 for Gal4 and oNS119 and oNS198 for *inc¹*. pUASTattB-based vectors generated in this study were integrated at *attP2* [25] with phiC31 recombinase (BestGene); integration was verified by PCR using primer attP2-5' paired with oNS277, oNS286, oNS288, or oNS290 for Inc, KCTD2, KCTD5, and KCTD17 respectively. All transgenes were backcrossed eight generations to Bloomington stock 5905, an isogenic *w¹¹¹⁸* stock described elsewhere as iso31 [77].

Sleep analysis

Crosses were set with five virgin females and three males on cornmeal, agar, and molasses food. One to four day old male flies eclosing from LD-entrained cultures raised at 25°C were loaded in glass tubes containing cornmeal, agar, and molasses food. Animals were monitored for 5–7 days at 25°C in LD cycles using DAM2 monitors (Trikinetics). The first 36–48 hours of data was discarded to permit animals to acclimate to glass tubes, and an integral number of days of data (3–5) were analyzed using custom Matlab software as described previously [11]. Locomotor data were collected in 1 min bins, and sleep was defined by inactivity for 5 minutes or more; a given minute was assigned as sleep if an animal was inactive for that minute and the preceding four minutes. Dead animals were excluded from analysis by a combination of automated filtering and visual inspection of locomotor traces.

Electrophysiology

Electrophysiological recordings were performed from abdominal segment 3 muscle 6/7 of third instar larvae as previously described [78].

Statistics

One-way ANOVA and Tukey post-hoc tests were used for comparisons of total sleep, daytime sleep, nighttime sleep, sleep bout number, and bouton number. Nonparametric Kruskal-Wallis tests and Dunn's post hoc tests were used for comparisons of sleep bout length. Unpaired two-sided Student's t-tests were used for comparisons of all electrophysiological parameters.

Sequence alignments

Alignments were performed with Clustal Omega 1.2.1 and BOXSHADE. GenBank accession numbers for transcript variants referred to in [S1](#) and [S2](#) Figs are: KCTD2, NM_183285; KCTD5, NM_027008; KCTD17.1, NM_001289671; KCTD17.2, NM_001289672; KCTD17.3, NM_001289673; KCTD17.4, NR_110357; KCTD17.v1, XM_006521460; KCTD17.v2, XM_011245739; KCTD17.v3, XM_011245740; KCTD17.v4, XM_011245741; KCTD17.v5, XM_006521461; KCTD17.v6, XM_006521462; KCTD17.v7, XM_011245742; KCTD17.v8, XM_006521465; hKCTD17.2, NM_024681.

Supporting information

S1 Fig. In situ hybridization for mouse *Insomniac* orthologs. (A) Allen Brain Atlas in situ hybridization images for KCTD2 and KCTD17. Brain regions with KCTD2 signal include cortex, hippocampus, striatum, thalamus, hypothalamus, cerebellum, pons, and medulla. KCTD17 signal is more sparse and is present in cortex, hippocampus, striatum, thalamus, and cerebellum. KCTD17 probe in these experiments is complementary to predicted KCTD17 transcript isoforms v1, v2, and v5 (see [S2 Fig](#) and [Materials and Methods](#)). (B) In situ hybridization of mouse coronal brain section using a probe complementary to KCTD17 transcript isoforms 1, 2, 3, 4, and predicted variants v2 and v4. Signal is prominent in the caudate putamen (CPu) and thalamus, as shown for the laterodorsal thalamic nucleus (LDDM) and laterodorsal ventrolateral thalamus (LDVL), but weak or absent from cortex (left panel), suggesting that cortical KCTD17 signal in (A) may reflect differential expression of a nonoverlapping subset of KCTD17 transcript isoforms.
(PDF)

S2 Fig. Sequence analysis of mouse *Insomniac* orthologs. (A) Alignment of Inc and its mouse orthologs. Conserved BTB and C-terminal domains are indicated. Identical and similar residues are shaded in black and gray, respectively. (B) Analysis of alternatively spliced forms of mouse KCTD17 (mKCTD17). mKCTD2, mKCTD5, and mKCTD17 isoforms encoded by brain cDNAs are shown at top; predicted mKCTD17 splice variants from GenBank that may be conserved in vertebrates are shown beneath (v1, v4, v8). Other predicted variants are not depicted (v2, v3, v5, v6, v7, see [Methods](#)). Expression of at least some of these predicted variants in brain is suggested by in situ hybridization ([S1A Fig](#)) but requires further characterization. Alternative splicing yields variant C-termini, with color indicating residues shared by different isoforms. The sequence of a human KCTD17 isoform (hKCTD17.2) characterized in Kasahara et al [[24](#)] is shown at bottom. Deletion of underlined hKCTD17.2 residues abolishes interaction with trichoplein. Note that residues implicated in binding trichoplein are absent in mKCTD2, mKCTD5, mKCTD17.2, mKCTD17.3, and Inc.
(PDF)

S3 Fig. Specificity of anti-KCTD5 antisera and co-immunoprecipitation of Cul3 and endogenous KCTD2/5/17. (A) Western blot of extracts from 293T cells transfected with indicated expression vectors and probed with anti-KCTD5. The first lane contains a control sample from cells transfected with empty vector and treated in parallel. Arrow indicates endogenous

species corresponding to KCTD 2/5/17. (B) 293T cells transfected and immunoprecipitated as indicated.

(PDF)

S4 Fig. Additional sleep parameters for animals expressing Inc and Inc orthologs. (A–D) Sleep parameters for animals expressing Inc and Inc orthologs panneuronally under *elav-Gal4* control.

n = 37–40 as in Fig 4C; * p < 0.01 compared to *elav-Gal4* control; ns, not significant (p > 0.05).

(E–H) Sleep parameters for *inc¹ inc-Gal4* animals expressing Inc and Inc orthologs. n = 18–157 as in Fig 4D. * p < 0.01 compared to *inc¹ inc-Gal4* animals, but not significantly different from wild-type control. ‡ p < 0.01 for comparisons to *inc¹ inc-Gal4* animals and to wild-type controls. For all panels, mean ± SEM is shown. (A and E) Nighttime sleep. (B and F) Daytime sleep. (C and G) Sleep bout length. (D and H) Sleep bout number. For all panels, animals are heterozygous for UAS transgenes.

(PDF)

S5 Fig. Localization of Insomniac family members in cultured cells. (A) Confocal micrographs of fixed S2 cell expressing 3×Myc-Inc (left panel), live S2 cell expressing Inc-GFP (middle panel), and fixed S2 cell expressing Inc-GFP (right panel). (B–D) Confocal micrographs of fixed 293T cells expressing indicated proteins bearing a 3×Myc tag (B), GFP tag (C), or 3×HA tag (D). Scale bar is 10 μM.

(PDF)

S6 Fig. Functional rescue of *inc* sleep phenotypes with 3×FLAG-Inc. 3×FLAG-Inc rescues sleep duration of *inc* mutants when expressed under *inc-Gal4* control. Animals are heterozygous for *UAS-3×FLAG-Inc*. n = 27–30, mean ± SEM is shown. * indicates not significantly different from wild-type animals and significantly different (p < 0.01) from *inc¹ inc-Gal4* control.

(PDF)

S7 Fig. Neuronal localization of Insomniac in vivo. (A) *inc-Gal4; UAS-nls-GFP / +* adult brain stained with anti-GFP and anti-PDF antibodies. (B–B') *pdf-Gal4; UAS-Myc-Inc / +* brain stained with anti-PDF (B) and anti-Myc (B') antibodies. Arrows and arrowhead indicate Myc-Inc signal in dorsal and contralateral projections, respectively. In (B'), inset at lower gain shows primarily extranuclear Myc-Inc signal within PDF⁺ neuron cell bodies. (C–C'') *pdf-Gal4; UAS-DenMark UAS-Syt-eGFP / +* brain stained with anti-GFP and anti-dsRed antibodies. (D) Magnified Z-projection of *crz-Gal4 / +; UAS-Myc-Inc / +* left brain hemisphere from Fig 6C is shown at lower gain. anti-Myc signal in CRZ⁺ neuron cell bodies is primarily extranuclear or perinuclear. Scale bars represent 10 μm in (A), 25 μm in (B), 50 μm in (C), and 25 μm in (D).

(PDF)

S8 Fig. Immunohistochemical analysis of Inc localization at NMJ 4 and in male larvae. (A) Confocal micrograph of NMJ 4 from a female third instar *inc-Gal4 / +; UAS-Myc-Inc / +* larva.

(B) Confocal micrograph of NMJ 6/7 from a male third instar *inc-Gal4; UAS-Myc-Inc / +* larva. Note higher level of Inc signal in muscle and HRP-negative trachea relative to larva shown in Fig 6F; this higher level of expression may reflect dosage compensation of the X-linked *inc-Gal4* transgene in hemizygous males versus heterozygous females, or sex-specific position effects of the X-linked *inc-Gal4* transgene insertion site.

(PDF)

Acknowledgments

We thank G. Fishell and R. Tsien for sharing facilities; B. Schulman for discussions of Cul3 adaptors; and J. Dasen, N. Ringstad, M. Shirasu-Hiza, J. Treisman, R. Tsien, and members of

the Stavropoulos lab for comments on the manuscript and discussions. N.S. thanks M. Young for support during the initiation of this work.

Author Contributions

Conceptualization: NS QL DAK HAMH TY CAF.

Formal analysis: QL DAK HAMH TY SS RPM CAF NS.

Funding acquisition: QL CAF NS.

Investigation: QL DAK HAMH TY SS RPM CAF NS.

Supervision: NS.

Visualization: QL DAK HAMH TY CAF NS.

Writing – original draft: NS.

Writing – review & editing: QL DAK HAMH TY RPM CAF NS.

References

1. Campbell SS, Tobler I. Animal sleep: a review of sleep duration across phylogeny. *Neurosci Biobehav Rev.* 1984; 8: 269–300. PMID: [6504414](#)
2. Joiner WJ. Unraveling the Evolutionary Determinants of Sleep. *Curr Biol.* 2016; 26: R1073–R1087. <https://doi.org/10.1016/j.cub.2016.08.068> PMID: [27780049](#)
3. Borbély AA. A two process model of sleep regulation. *Hum Neurobiol.* 1982; 1: 195–204. PMID: [7185792](#)
4. Young MW, Kay SA. Time zones: a comparative genetics of circadian clocks. *Nat Rev Genet.* 2001; 2: 702–715. <https://doi.org/10.1038/35088576> PMID: [11533719](#)
5. Lowrey PL, Takahashi JS. Genetics of circadian rhythms in Mammalian model organisms. *Adv Genet.* 2011; 74: 175–230. <https://doi.org/10.1016/B978-0-12-387690-4.00006-4> PMID: [21924978](#)
6. Reddy P, Zehring WA, Wheeler DA, Pirrotta V, Hadfield C, Hall JC, et al. Molecular analysis of the period locus in *Drosophila melanogaster* and identification of a transcript involved in biological rhythms. *Cell.* 1984; 38: 701–710. PMID: [6435882](#)
7. Bargiello TA, Jackson FR, Young MW. Restoration of circadian behavioural rhythms by gene transfer in *Drosophila*. *Nature.* 1984; 312: 752–754. PMID: [6440029](#)
8. Kloss B, Price JL, Saez L, Blau J, Rothenfluh A, Wesley CS, et al. The *Drosophila* clock gene double-time encodes a protein closely related to human casein kinase Iepsilon. *Cell.* 1998; 94: 97–107. PMID: [9674431](#)
9. Toh KL, Jones CR, He Y, Eide EJ, Hinz WA, Virshup DM, et al. An hPer2 phosphorylation site mutation in familial advanced sleep phase syndrome. *Science.* 2001; 291: 1040–1043. PMID: [11232563](#)
10. Xu Y, Padiath QS, Shapiro RE, Jones CR, Wu SC, Saigoh N, et al. Functional consequences of a CKI-delta mutation causing familial advanced sleep phase syndrome. *Nature.* 2005; 434: 640–644. <https://doi.org/10.1038/nature03453> PMID: [15800623](#)
11. Stavropoulos N, Young MW. *insomniac* and *Cullin-3* regulate sleep and wakefulness in *Drosophila*. *Neuron.* 2011; 72: 964–976. <https://doi.org/10.1016/j.neuron.2011.12.003> PMID: [22196332](#)
12. Pfeifferberger C, Allada R. *Cul3* and the BTB adaptor *insomniac* are key regulators of sleep homeostasis and a dopamine arousal pathway in *Drosophila*. *PLoS Genet.* 2012; 8: e1003003. <https://doi.org/10.1371/journal.pgen.1003003> PMID: [23055946](#)
13. Stogios PJ, Downs GS, Jauhal JJS, Nandra SK, Privé GG. Sequence and structural analysis of BTB domain proteins. *Genome Biol.* 2005; 6: R82. <https://doi.org/10.1186/gb-2005-6-10-r82> PMID: [16207353](#)
14. Xu L, Wei Y, Reboul J, Vaglio P, Shin T-H, Vidal M, et al. BTB proteins are substrate-specific adaptors in an SCF-like modular ubiquitin ligase containing *CUL-3*. *Nature.* 2003; 425: 316–321. <https://doi.org/10.1038/nature01985> PMID: [13679922](#)

15. Pintard L, Willis JH, Willems A, Johnson J-LF, Srayko M, Kurz T, et al. The BTB protein MEL-26 is a substrate-specific adaptor of the CUL-3 ubiquitin-ligase. *Nature*. 2003; 425: 311–316. <https://doi.org/10.1038/nature01959> PMID: 13679921
16. Geyer R, Wee S, Anderson S, Yates J, Wolf DA. BTB/POZ domain proteins are putative substrate adaptors for cullin 3 ubiquitin ligases. *Mol Cell*. 2003; 12: 783–790. PMID: 14527422
17. Furukawa M, He YJ, Borchers C, Xiong Y. Targeting of protein ubiquitination by BTB-Cullin 3-Roc1 ubiquitin ligases. *Nat Cell Biol*. 2003; 5: 1001–1007. <https://doi.org/10.1038/ncb1056> PMID: 14528312
18. Zhuang M, Calabrese MF, Liu J, Waddell MB, Nourse A, Hammel M, et al. Structures of SPOP-substrate complexes: insights into molecular architectures of BTB-Cul3 ubiquitin ligases. *Mol Cell*. 2009; 36: 39–50. <https://doi.org/10.1016/j.molcel.2009.09.022> PMID: 19818708
19. Errington WJ, Khan MQ, Bueler SA, Rubinstein JL, Chakrabarty A, Privé GG. Adaptor protein self-assembly drives the control of a cullin-RING ubiquitin ligase. *Structure*. 2012; 20: 1141–1153. <https://doi.org/10.1016/j.str.2012.04.009> PMID: 22632832
20. Bayón Y, Trinidad AG, la Puerta de ML, Del Carmen Rodríguez M, Bogetz J, Rojas A, et al. KCTD5, a putative substrate adaptor for cullin3 ubiquitin ligases. *FEBS J*. 2008; 275: 3900–3910. <https://doi.org/10.1111/j.1742-4658.2008.06537.x> PMID: 18573101
21. Dementieva IS, Tereshko V, McCrossan ZA, Solomaha E, Araki D, Xu C, et al. Pentameric assembly of potassium channel tetramerization domain-containing protein 5. *J Mol Biol*. 2009; 387: 175–191. <https://doi.org/10.1016/j.jmb.2009.01.030> PMID: 19361449
22. Weger S, Hammer E, Götz A, Heilbronn R. Identification of a cytoplasmic interaction partner of the large regulatory proteins Rep78/Rep68 of adeno-associated virus type 2 (AAV-2). *Virology*. 2007; 362: 192–206. <https://doi.org/10.1016/j.virol.2006.12.010> PMID: 17239418
23. Rutz N, Heilbronn R, Weger S. Interactions of cullin3/KCTD5 complexes with both cytoplasmic and nuclear proteins: Evidence for a role in protein stabilization. *Biochem Biophys Res Commun*. 2015; 464: 922–928. <https://doi.org/10.1016/j.bbrc.2015.07.069> PMID: 26188516
24. Kasahara K, Kawakami Y, Kiyono T, Yonemura S, Kawamura Y, Era S, et al. Ubiquitin-proteasome system controls ciliogenesis at the initial step of axoneme extension. *Nat Comms*. 2014; 5: 5081.
25. Groth AC, Fish M, Nusse R, Calos MP. Construction of transgenic *Drosophila* by using the site-specific integrase from phage phiC31. *Genetics*. 2004; 166: 1775–1782. PMID: 15126397
26. Cirelli C, Bushey D, Hill S, Huber R, Kreber R, Ganetzky B, et al. Reduced sleep in *Drosophila* Shaker mutants. *Nature*. 2005; 434: 1087–1092. <https://doi.org/10.1038/nature03486> PMID: 15858564
27. Zimmerman JE, Chan MT, Jackson N, Maislin G, Pack AI. Genetic background has a major impact on differences in sleep resulting from environmental influences in *Drosophila*. *Sleep*. 2012; 35: 545–557. <https://doi.org/10.5665/sleep.1744> PMID: 22467993
28. Ganguly-Fitzgerald I, Donlea J, Shaw PJ. Waking experience affects sleep need in *Drosophila*. *Science*. 2006; 313: 1775–1781. <https://doi.org/10.1126/science.1130408> PMID: 16990546
29. Itoh K, Wakabayashi N, Katoh Y, Ishii T, Igarashi K, Engel JD, et al. Keap1 represses nuclear activation of antioxidant responsive elements by Nrf2 through binding to the amino-terminal Neh2 domain. *Genes Dev*. 1999; 13: 76–86. PMID: 9887101
30. Nagai Y, Kojima T, Muro Y, Hachiya T, Nishizawa Y, Wakabayashi T, et al. Identification of a novel nuclear speckle-type protein, SPOP. *FEBS Letters*. 1997; 418: 23–26. PMID: 9414087
31. Xue F, Cooley L. kelch encodes a component of intercellular bridges in *Drosophila* egg chambers. *Cell*. 1993; 72: 681–693. PMID: 8453663
32. Maerki S, Olma MH, Staubli T, Steigemann P, Gerlich DW, Quadroni M, et al. The Cul3-KLHL21 E3 ubiquitin ligase targets aurora B to midzone microtubules in anaphase and is required for cytokinesis. *J Cell Biol*. 2009; 187: 791–800. <https://doi.org/10.1083/jcb.200906117> PMID: 19995937
33. Schaefer H, Rongo C. KEL-8 is a substrate receptor for CUL3-dependent ubiquitin ligase that regulates synaptic glutamate receptor turnover. *Mol Biol Cell*. 2006; 17: 1250–1260. <https://doi.org/10.1091/mbc.E05-08-0794> PMID: 16394099
34. Choi YJ, Lee G, Hall JC, Park JH. Comparative analysis of Corazonin-encoding genes (Crz's) in *Drosophila* species and functional insights into Crz-expressing neurons. *J Comp Neurol*. 2005; 482: 372–385. <https://doi.org/10.1002/cne.20419> PMID: 15669053
35. Renn SC, Park JH, Rosbash M, Hall JC, Taghert PH. A pdf neuropeptide gene mutation and ablation of PDF neurons each cause severe abnormalities of behavioral circadian rhythms in *Drosophila*. *Cell*. 1999; 99: 791–802. PMID: 10619432
36. Zhang YQ, Rodesch CK, Broadie K. Living synaptic vesicle marker: synaptotagmin-GFP. *Genesis*. 2002; 34: 142–145. <https://doi.org/10.1002/gen.10144> PMID: 12324970

37. Nicolaï LJJ, Ramaekers A, Raemaekers T, Drozdzecki A, Mauss AS, Yan J, et al. Genetically encoded dendritic marker sheds light on neuronal connectivity in *Drosophila*. *Proc Natl Acad Sci USA*. 2010; 107: 20553–20558. <https://doi.org/10.1073/pnas.1010198107> PMID: 21059961
38. Helfrich-Förster C, Shafer OT, Wülbeck C, Grieshaber E, Rieger D, Taghert P. Development and morphology of the clock-gene-expressing lateral neurons of *Drosophila melanogaster*. *J Comp Neurol*. 2007; 500: 47–70. <https://doi.org/10.1002/cne.21146> PMID: 17099895
39. Menon KP, Carrillo RA, Zinn K. Development and plasticity of the *Drosophila* larval neuromuscular junction. *Wiley Interdiscip Rev Dev Biol*. 2013; 2: 647–670. <https://doi.org/10.1002/wdev.108> PMID: 24014452
40. Tononi G, Cirelli C. Sleep and synaptic homeostasis: a hypothesis. *Brain Res Bull*. 2003; 62: 143–150. PMID: 14638388
41. Vyazovskiy VV, Cirelli C, Pfister-Genskow M, Faraguna U, Tononi G. Molecular and electrophysiological evidence for net synaptic potentiation in wake and depression in sleep. *Nat Neurosci*. 2008; 11: 200–208. <https://doi.org/10.1038/nn2035> PMID: 18204445
42. Donlea JM, Ramanan N, Shaw PJ. Use-dependent plasticity in clock neurons regulates sleep need in *Drosophila*. *Science*. 2009; 324: 105–108. <https://doi.org/10.1126/science.1166657> PMID: 19342592
43. Gilestro GF, Tononi G, Cirelli C. Widespread changes in synaptic markers as a function of sleep and wakefulness in *Drosophila*. *Science*. 2009; 324: 109–112. <https://doi.org/10.1126/science.1166673> PMID: 19342593
44. Bushey D, Tononi G, Cirelli C. Sleep and synaptic homeostasis: structural evidence in *Drosophila*. *Science*. 2011; 332: 1576–1581. <https://doi.org/10.1126/science.1202839> PMID: 21700878
45. Yang G, Lai CSW, Cichon J, Ma L, Li W, Gan W-B. Sleep promotes branch-specific formation of dendritic spines after learning. *Science*. 2014; 344: 1173–1178. <https://doi.org/10.1126/science.1249098> PMID: 24904169
46. Allada R, Siegel JM. Unearthing the phylogenetic roots of sleep. *Curr Biol*. 2008; 18: R670–R679. <https://doi.org/10.1016/j.cub.2008.06.033> PMID: 18682212
47. Duda DM, Scott DC, Calabrese MF, Zimmerman ES, Zheng N, Schulman BA. Structural regulation of cullin-RING ubiquitin ligase complexes. *Curr Opin Struct Biol*. 2011; 21: 257–264. <https://doi.org/10.1016/j.sbi.2011.01.003> PMID: 21288713
48. Zhang Q, Zhang L, Wang B, Ou C-Y, Chien C-T, Jiang J. A hedgehog-induced BTB protein modulates hedgehog signaling by degrading Ci/Gli transcription factor. *Dev Cell*. 2006; 10: 719–729. <https://doi.org/10.1016/j.devcel.2006.05.004> PMID: 16740475
49. Yi JJ, Ehlers MD. Ubiquitin and protein turnover in synapse function. *Neuron*. 2005; 47: 629–632. <https://doi.org/10.1016/j.neuron.2005.07.008> PMID: 16129392
50. Patrick GN. Synapse formation and plasticity: recent insights from the perspective of the ubiquitin proteasome system. *Curr Opin Neurobiol*. 2006; 16: 90–94. <https://doi.org/10.1016/j.conb.2006.01.007> PMID: 16427269
51. Haas KF, Broadie K. Roles of ubiquitination at the synapse. *Biochim Biophys Acta*. 2008; 1779: 495–506. <https://doi.org/10.1016/j.bbagen.2007.12.010> PMID: 18222124
52. Mabb AM, Ehlers MD. Ubiquitination in postsynaptic function and plasticity. *Annu Rev Cell Dev Biol*. 2010; 26: 179–210. <https://doi.org/10.1146/annurev-cellbio-100109-104129> PMID: 20604708
53. Bushey D, Tononi G, Cirelli C. The *Drosophila* fragile X mental retardation gene regulates sleep need. *Journal of Neuroscience*. 2009; 29: 1948–1961. <https://doi.org/10.1523/JNEUROSCI.4830-08.2009> PMID: 19228950
54. Robinson JE, Paluch J, Dickman DK, Joiner WJ. ADAR-mediated RNA editing suppresses sleep by acting as a brake on glutamatergic synaptic plasticity. *Nat Comms*. 2016; 7: 10512.
55. Pan L, Zhang YQ, Woodruff E, Broadie K. The *Drosophila* fragile X gene negatively regulates neuronal elaboration and synaptic differentiation. *Curr Biol*. 2004; 14: 1863–1870. <https://doi.org/10.1016/j.cub.2004.09.085> PMID: 15498496
56. Tessier CR, Broadie K. *Drosophila* fragile X mental retardation protein developmentally regulates activity-dependent axon pruning. *Development*. 2008; 135: 1547–1557. <https://doi.org/10.1242/dev.015867> PMID: 18321984
57. Bushey D, Huber R, Tononi G, Cirelli C. *Drosophila* Hyperkinetic mutants have reduced sleep and impaired memory. *Journal of Neuroscience*. 2007; 27: 5384–5393. <https://doi.org/10.1523/JNEUROSCI.0108-07.2007> PMID: 17507560
58. Jan YN, Jan LY, Dennis MJ. Two mutations of synaptic transmission in *Drosophila*. *Proc R Soc Lond, B, Biol Sci*. 1977; 198: 87–108. PMID: 20636

59. Stern M, Ganetzky B. Altered synaptic transmission in *Drosophila* hyperkinetic mutants. *Journal of neurogenetics*. 1989; 5: 215–228. PMID: [2553904](#)
60. Budnik V, Zhong Y, Wu C-F. Morphological plasticity of motor axons in *Drosophila* mutants with altered excitability. *J Neurosci*. 1990; 10: 3754–3768. PMID: [1700086](#)
61. Li Q, Stavropoulos N. Evaluation of Ligand-Inducible Expression Systems for Conditional Neuronal Manipulations of Sleep in *Drosophila*. *G3: Genes | Genomes | Genetics*. 2016; 6: 3351–3359. <https://doi.org/10.1534/g3.116.034132> PMID: [27558667](#)
62. Singh K, Ju JY, Walsh MB, Dilorio MA, Hart AC. Deep conservation of genes required for both *Drosophila melanogaster* and *Caenorhabditis elegans* sleep includes a role for dopaminergic signaling. *Sleep*. 2014; 37: 1439–1451. <https://doi.org/10.5665/sleep.3990> PMID: [25142568](#)
63. Boada M, Antúnez C, Ramírez-Lorca R, DeStefano AL, González-Pérez A, Gayán J, et al. ATP5H/KCTD2 locus is associated with Alzheimer's disease risk. *Molecular Psychiatry*. 2014; 19: 682–687. <https://doi.org/10.1038/mp.2013.86> PMID: [23857120](#)
64. Mencacci NE, Rubio-Agusti I, Zdebek A, Asmus F, Ludtmann MHR, Ryten M, et al. A missense mutation in KCTD17 causes autosomal dominant myoclonus-dystonia. *American journal of human genetics*. 2015; 96: 938–947. <https://doi.org/10.1016/j.ajhg.2015.04.008> PMID: [25983243](#)
65. O'Roak BJ, Vives L, Girirajan S, Karakoc E, Krumm N, Coe BP, et al. Sporadic autism exomes reveal a highly interconnected protein network of de novo mutations. *Nature*. 2012; 485: 246–250. <https://doi.org/10.1038/nature10989> PMID: [22495309](#)
66. Kong A, Frigge ML, Masson G, Besenbacher S, Sulem P, Magnusson G, et al. Rate of de novo mutations and the importance of father's age to disease risk. *Nature*. 2012; 488: 471–475. <https://doi.org/10.1038/nature11396> PMID: [22914163](#)
67. Codina-Solà M, Rodríguez-Santiago B, Homs A, Santoyo J, Rigau M, Aznar-Laín G, et al. Integrated analysis of whole-exome sequencing and transcriptome profiling in males with autism spectrum disorders. *Mol Autism*. 2015; 6: 21. <https://doi.org/10.1186/s13229-015-0017-0> PMID: [25969726](#)
68. Souders MC, Mason TBA, Valladares O, Bućan M, Levy SE, Mandell DS, et al. Sleep behaviors and sleep quality in children with autism spectrum disorders. *Sleep*. 2009; 32: 1566–1578. PMID: [20041592](#)
69. Bourgeron T. From the genetic architecture to synaptic plasticity in autism spectrum disorder. *Nat Rev Neurosci*. 2015; 16: 551–563. <https://doi.org/10.1038/nrn3992> PMID: [26289574](#)
70. Lee S, Hjerling-Leffler J, Zaghera E, Fishell G, Rudy B. The largest group of superficial neocortical GABAergic interneurons expresses ionotropic serotonin receptors. *Journal of Neuroscience*. 2010; 30: 16796–16808. <https://doi.org/10.1523/JNEUROSCI.1869-10.2010> PMID: [21159951](#)
71. Bischof J, Maeda RK, Hediger M, Karch F, Basler K. An optimized transgenesis system for *Drosophila* using germ-line-specific C31 integrases. *Proc Natl Acad Sci USA*. 2007; 104: 3312–3317. <https://doi.org/10.1073/pnas.0611511104> PMID: [17360644](#)
72. Ma H, Groth RD, Cohen SM, Emery JF, Li B, Hoedt E, et al. γ CaMKII shuttles Ca^{2+} /CaM to the nucleus to trigger CREB phosphorylation and gene expression. *Cell*. 2014; 159: 281–294. <https://doi.org/10.1016/j.cell.2014.09.019> PMID: [25303525](#)
73. Carlin RK, Grab DJ, Cohen RS, Siekevitz P. Isolation and characterization of postsynaptic densities from various brain regions: enrichment of different types of postsynaptic densities. *J Cell Biol*. 1980; 86: 831–845. PMID: [7410481](#)
74. Veenstra JA, Davis NT. Localization of corazonin in the nervous system of the cockroach *Periplaneta americana*. *Cell Tissue Res*. 1993; 274: 57–64. PMID: [8242711](#)
75. Kerkis J. The Growth of the Gonads in *DROSOPHILA MELANOGASTER*. *Genetics*. 1931; 16: 212–224. PMID: [17246617](#)
76. Lin DM, Goodman CS. Ectopic and increased expression of Fasciclin II alters motoneuron growth cone guidance. *Neuron*. 1994; 13: 507–523. PMID: [7917288](#)
77. Ryder E, Blows F, Ashburner M, Bautista-Llacer R, Coulson D, Drummond J, et al. The DrosDel collection: a set of P-element insertions for generating custom chromosomal aberrations in *Drosophila melanogaster*. *Genetics*. 2004; 167: 797–813. <https://doi.org/10.1534/genetics.104.026658> PMID: [15238529](#)
78. Spring AM, Brusich DJ, Frank CA. C-terminal Src Kinase Gates Homeostatic Synaptic Plasticity and Regulates Fasciclin II Expression at the *Drosophila* Neuromuscular Junction. *PLoS Genet*. 2016; 12: e1005886. <https://doi.org/10.1371/journal.pgen.1005886> PMID: [26901416](#)